UNIVERSITAT POLITÈCNICA DE CATALUNYA

III Engineering Faculty

Master of science in Telecommunication Engineering

Master Thesis

PMD IMPAIRMENTS IN OPTICAL FIBER TRANSMISSION AT 10 GBPS AND 40 GBPS

Student: **Alessandro Pilichi**

Spanish coordinator: **Gabriel Junyent**
Italian coordinator: **Roberto Gaudino**

Turin, 9 November 2010
Barcelona, 24 November 2010

A mio padre, mia madre e mia sorella
per avermi sempre sostenuto, aiutato e voluto bene

Abstract

The continuous need for greater bandwidth and capacity to support existing and emerging technologies, such as fiber-to-the-home (FTTH) and Internet Protocol Television(IPTV), drive optical-communication systems to higher and higher data rates per wavelength channel, from 10 to 40 Gbps and above. Degrading effects that tended to cause non catastrophic events at lower bit rates have become critical concerns for high-performance networks. Among them, polarization-mode dispersion (PMD) is perhaps the largest concern and, therefore, has garnered a great amount of attention.

The PMD arises in an optical fiber from asymmetries in the fiber core that induce a small amount of birefringence that randomly varies along the length of the fiber. This birefringence causes the power in each optical pulse to split between the two polarization modes of the fiber and travel at different speeds, creating a differential group delay (DGD) between the two modes that can result in pulse spreading and intersymbol interference. PMD becomes a unique and challenging hurdle for high-performance systems mainly due to its dynamic and random nature. The polarization state is generally unknown and wanders with time. In general, PMD effects are wavelength (channel) dependent and can vary over a time scale of milliseconds. As a random variable, the DGD follows a Maxwellian distribution for which high-DGD points in the tail of the distribution can lead to network outages.

Typically, system designers require the outage probability for high-performance networks to be 10−5 or less (penalty > 1dB for <30 min/yr). Clearly, the most straightforward approach to overcoming the effects of PMD is to employ newly manufactured low-PMD optical fibers, which have PMD values < $0.1 ps/\sqrt{Km}$.

However, much of the previously embedded fiber has high PMD values between 0.5 and 1 $ps/\sqrt{Km}$ or even higher. The reality of deploying new systems over the embedded fiber means that the PMD monitoring and compensation are important for PMD mitigation. Unlike other degrading effects such as chromatic dispersion, the PMD is a time-varying random process making compensation difficult.

Abstract

The aim of this work is to study the trend of PMD effects over two different system, at 10 and 40 Gbps with two kind of fiber with high (0.5 $^{ps}/_{\sqrt{Km}}$) and low (0.1 $^{ps}/_{\sqrt{Km}}$) PMD coefficient. The first one corresponds to an old fiber's type, that is used in the majority in the current transmission system; while the second one corresponds to a new fiber's type, designed to have a lower response to the PMD phenomenon, making possible the transmission over long distances at high bit-rates.

This work is structured as follows:

After a short introduction, the second chapter is a review of PMD theory; where the PMD is faced from a theoretical point of view. It's reported how the PMD arises in a fiber, how the DGD has a Maxwellian probability distribution, and the outage limits to design a system under the influences of PMD.

In the third chapter there is a literary review over the PMD mitigation. Over the years, research groups from around the globe have proposed and/or demonstrated different strategies for PMD compensation. In this chapter an overview of these strategies shall be given, mentioning their relative merits and demerits. Following that, methods to increase the tolerance of a fiber-optic communication system to PMD, will also be discussed.

After this theoretical introduction the central part's of this study starts. In the fourth chapter the limitations imposed by the PMD are investigated.
We starts probing the theoretical distance limits imposed by the only PMD, setting all other fiber's impairments and attenuation to be negligible. Sequentially two single span optical transmission systems are compared on the basis of fiber PMD coefficient and bit-rates, to find the maximum distance that can be reached with a bit error rate of 10^{-10}, taking in account or not the PMD and setting only the attenuation of the fiber. After this first investigation, the real impact of PMD was reported, performing a simulation of a multi span system, where the fiber's attenuation of each section is compensated by an amplifier, so to find the maximum reachable distances over long-haul transmission and clearly see how is the PMD impact.

In the last chapter a first-order polarization compensator is tested. Firstly in order to show how the compensator could works, the monitor signal's simulation (based on the analysis of the Power Spectral Densities at selected frequency) is made, to show how the PMD level is related to the PSD. After that, the compensator is tested, performing two simulations at 10 and 40 Gbps with different value of DGD reached at the end of the fiber, to demonstrate the real capability of the compensator.

The last study done is over the compensation applied to the previous multi-span system, to study how the performance of a system get increasing with a PMD compensation, and what is the system tolerance to PMD with or without compensation.

All the simulation of this work are made with the use of a software package (1) used in the optical laboratory of *Universitat Politècnica de Catalunya*.

CONTENTS

CHAPTER 1
INTRODUCTION

In spite of the recent telecom bubble, statistics show that the net traffic growth (combined Internet, data and voice traffic) remains at the same level as it was four years ago and network capacity is being exhausted at the same rate as it was during the pre-bubble time. Applications such as videoconference, telephony, movies on demand, distance learning, telemedicine and technologies like fiber-to-the-home (FTTH) and fiber-to-the-premise (FTTP) are expected to fuel the future bandwidth demand and soon the existing infrastructure will run out of capacity and new capacity will have to be added to accommodate the ever-growing need for bandwidth. One way to add capacity is to increase the transmission speeds. However, certain technical challenges need to be addressed to enable long-haul high-speed transmission. Two such challenges are polarization-mode dispersion (PMD) and chromatic dispersion variability, and of these two, PMD is the more difficult one because of its stochastic nature. While there are PMD challenges facing carriers at 10 Gb/s, these challenges are not as severe as originally feared. A marked improvement in the PMD tolerance of 10 Gb/s long-reach receivers will likely satisfy most length demands, obviating the need for PMD mitigation in many systems. However, transmission speeds of 40 Gb/s and beyond will most likely require some form of PMD mitigation in long-haul applications.

PMD is caused by optical birefringence and is a fundamental property of single-mode optical fiber and fiber-optic components in which signal energy at a wavelength is resolved into two orthogonal polarization modes of slightly different propagation velocities. PMD results in pulse broadening and distortion thereby leading to system performance degradation. Unlike the chromatic dispersion, PMD varies stochastically in time making it particularly difficult to assess, counter or cope with. Active research is being conducted by different groups on different issues of PMD for more than a decade. The key issues of PMD research can be broadly classified into three categories: (i) fundamental understanding of the phenomenon and its impact, (ii) measurement, and (iii)

mitigation strategies. The objective of the PMD research is to understand the stochastic nature of PMD thoroughly through analytical analysis, simulations and/or analysis of measured data and determine an efficient means for mitigating PMD effects on long-haul fiber networks. To ensure signal quality on their fiber at higher rates, network engineers must anticipate the impact of PMD on various fiber routes. Design of a reliable network requires a good model of the PMD characteristics on each link. An understanding of the temporal and spectral variability of both the differential group delay (DGD) and principal states of polarization (PSPs) is required to specify appropriate transmission parameters and also the required speed of PMD compensators. Factors such as the mean DGD, PMD correlation time and bandwidth, as well as second-order effects together with performance prediction models can provide this understanding. Also, a solid understanding of PMD-induced system outages will help engineers and researchers to develop new and cost-efficient mitigation alternatives to PMD compensators.

CHAPTER 2
POLARIZATION MODE DISPERSION

2.1 PMD FONDAMENTALS

Polarization mode dispersion (PMD) is a form of modal dispersion where two different polarizations of light in a waveguide, which normally travel at the same speed, travel at different speeds due to random imperfections and asymmetries, causing random spreading of optical pulses. Unless it is compensated, which is difficult, this ultimately limits the rate at which data can be transmitted over a fiber.

In an ideal optical fiber, the core has a perfectly circular cross-section. In this case, the fundamental mode has two orthogonal polarizations (orientations of the electric field) that travel at the same speed. The signal that is transmitted over the fiber is randomly polarized, i.e. a random superposition of these two polarizations, but that would not matter in an ideal fiber because the two polarizations would propagate identically.

In a realistic fiber, however, there are random imperfections that break the circular symmetry, causing the two polarizations to propagate with different speeds. In this case, the two polarization components of a signal will slowly separate, e.g. causing pulses to spread and overlap. Because the imperfections are random, the pulse spreading effects correspond to a random walk, and thus have a mean polarization-dependent time-differential Δτ (also called the differential group delay, or DGD) proportional to the square root of propagation distance L:

$$\Delta\tau = D_{PMD}\sqrt{L} \qquad \textbf{2.1}$$

Where D_{PMD} is the PMD parameter of the fiber, typically measured in ps/√km, a measure of the strength and frequency of the imperfections.

The symmetry-breaking random imperfections fall into several categories. First, there is geometric asymmetry, e.g. slightly elliptical cores. Second, there are stress-induced material birefringences, in which the refractive index itself depends on the polarization. Both of these effects can stem from either imperfection in manufacturing (which is never perfect or stress-free) or from thermal and mechanical stresses imposed on the fiber in the field moreover, the latter stresses generally vary over time.

2.2 **Birefringence in Optical Fibers**

In optical fiber communication systems, although we call the optical fiber as single mode fiber (SMF), there actually exist two orthogonally polarized HE11 modes. If the fiber has not only perfectly symmetric core and cladding geometry but also perfectly isotropic material, these two modes have the same group delay. However, in the real world, symmetry of the fibers is broken according to the internal perturbation and/or the external perturbation. So that the degeneracy of the two orthogonally polarized modes is broken: birefringence exists, or in other words the phase and group velocities of the two modes are different.

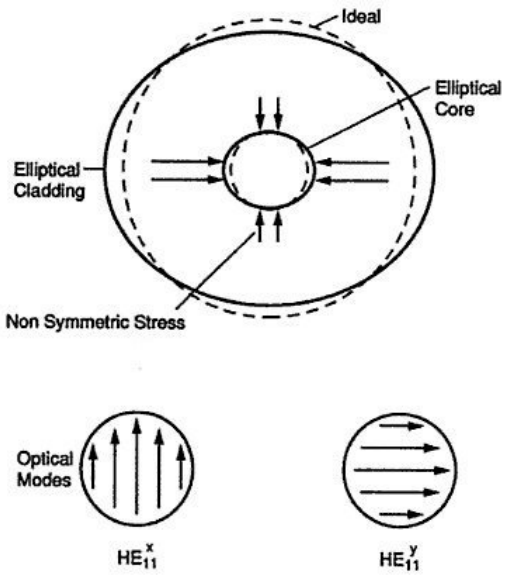

2.1 Figure anatomy of a real fibre

The internal perturbation comes from the manufacturing process and has two kinds. One kind is that the core is elliptical. In this case, geometric birefringence arises and the two HE11 modes have different propagation constants. The other kind is that though the core is circular, there exist asymmetric internal stress, which causes the material density difference, and thus the difference of the propagation constant of the two modes (1; 2)

The external perturbation includes Lateral stress, bending, and twist. The first two have the similar effects as the internal asymmetric stress, so they cause linear birefringence by introducing material density difference. Unlike all the other perturbation, fiber twist creates circular birefringence.

The birefringence of single mode fibers is on the order of $10^{-5} - 10^{-7}$, which is small compared to the refractive index of the core (~1.5), but in the long communication optical fiber it can cause large differential group delay between fast mode and slow mode compared to the pulse width of optical signal. The perturbation on single mode fiber is randomly distributed along the length. Ideally, in a short section of single mode fiber, the birefringence can be considered uniform. In this case, it can be viewed as a wave plate.

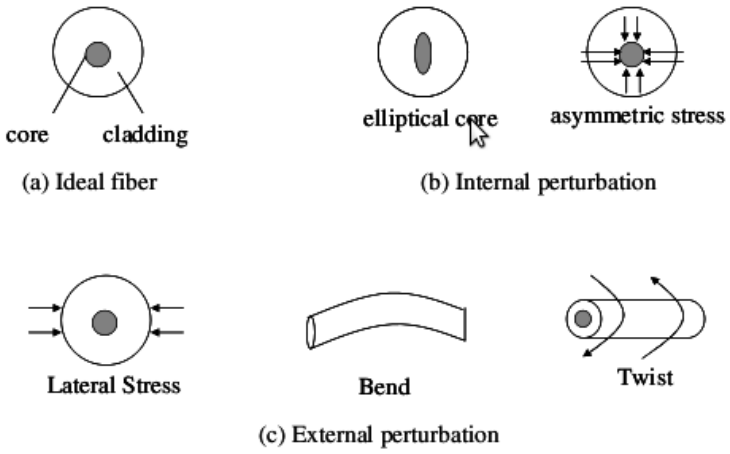

2.2 Different type of perturbation

The slow mode and the fast mode have difference in the propagation constant:

$$\frac{\Delta\tau}{L} = \frac{d}{d\omega}(\beta_{SLOW} - \beta_{FAST}) = \frac{\Delta n_{eff}}{c} - \frac{\omega d\Delta n_{eff}}{d\omega} \qquad 2.2$$

Where c is the speed of light, ω is the angular frequency of light, $n_{eff} = n_{fast} - n_{slow}$ and n_{slow}, n_{fast} are the effective refractive index of the slow mode and the fast mode respectively; we can see that the first term is independent of frequency and the second term is the dispersion of Δn.

The linear dependence of PMD could be applied only to short fibers length where the birefringence can be assumed to be uniform; instead of long-length fiber where the PMD has a square root of length dependence.

If the input wave is linearly polarized along the birefringence axis, only one mode is excited, and the SOP is maintained along the length of the fiber. Otherwise, both of the fast and slow modes are excited, and the input SOP is decomposed to the two modes which are orthogonal; as shows in Fig. 2.3.

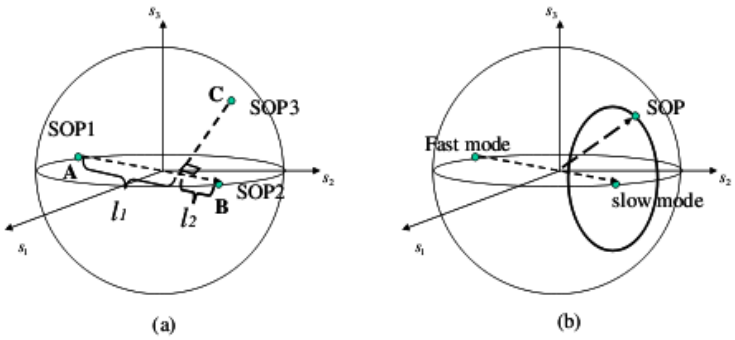

Figure 2.3 (A) Decompose a sop to an orthogonal sop pair. (b)Sop on a circle on the poincarè sphere.

Point A and point B denote the two orthogonal modes SOP1 and SOP2 on Poincarè sphere, and they are symmetric about the sphere centre. Point C denotes an arbitrary SOP3.

If we project C on the section AB, and cut it into two sections with length l_1 and l_2, we get this relation:

$$E_3 = a_1 e^{(i\varphi_1)} E_1 + a_2 e^{(j\varphi_2)} E_2 \qquad 2.3$$

$$\frac{a_1^2}{a_2^2} = \frac{l_2}{l_1} \qquad 2.4$$

where the Jones vector of SOP3 is written as the combinations of this orthogonal pair. The intensity ratio of each components is determined by the ratio of l_1 and l_2. With fixed intensity ratio, if the phase difference of the two components changes, SOP3 evolves on a circle. We know that as the two excited mode propagate along the fiber, the phase difference between them increases while the intensity ratio remains the same. So the SOP evolves on the circle with line AB as its axis and return to its original SOP after a length named “Beat Length” along the fiber (3).

The beat length is:

$$L_B = \frac{2\pi}{\beta_{slow} - \beta_{fast}} = \frac{2\pi}{\omega \Delta n / c} = \frac{\lambda}{\Delta n} \qquad 2.5$$

For 1550nm wavelength and $\Delta n \sim 10^{-7}$, the beat length is ~ 15m.

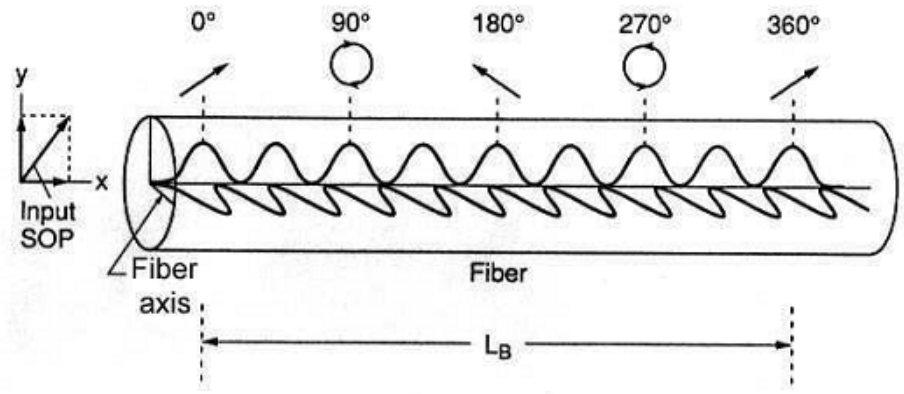

Figure 2.4 Beat length

If the input SOP is fixed, but the light frequency varies, the output SOP for a fixed length short fiber evolves in a similar way. In the case that only one mode is excited, then the output SOP from this ideal short birefringence maintains the same with the input SOP for all frequencies. While when two modes are excited, the output SOP traces the circle on the Poincarè sphere surface as the frequency is varied. The circle also has line AB as its axis.

2.3 **Polarization-Mode Coupling long-length**

In the short length of single mode fiber, where the perturbation is considered uniform, the DGD is deterministic. However, in the long-haul optical fiber communication system, the perturbation on fiber is random. Not only the scale of the birefringence is not uniform, but also the axes of the birefringence are random. These random axes cause polarization mode coupling. The slow and fast polarization modes from one segment are both decomposed to the slow and fast mode in the next segment (4). People use the concatenation of wave plates with random oriented birefringence axes to model this long fiber, as shown in Fig. 2.5.

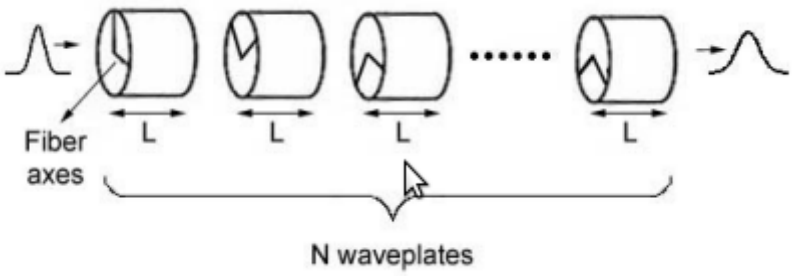

Figure 2.5 Model long fibers by concatenation of wave plates with birefringence oriented randonly along the fiber length

In such a long fiber, DGD does not accumulate linearly with fiber length. The pulse launched in fiber is splitted into two orthogonal pulses that continues down the waveguide with different velocities until they arrive at the next

perturbation where both pulses became split and form four pulses. This splitting of the pulses continues as more and more perturbations are encountered until there are a large number of small pulses propagating down the waveguide. Because the relative distance traveled in the two modes is different for each pulse, the arrival times of the pulses at the output are different. The result is that the optical energy of the input pulse becomes dispersed in time at the output Fig. 2.6.

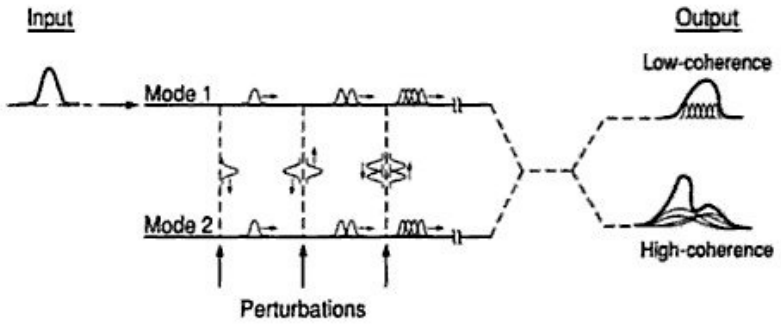

Figure 2.6 Pulse Propagation in a two-mode waveguide with random perturbations.

PMD in long fiber spans is a special case of the general problem of modal dispersion in a multimode waveguide subjected to random perturbations. In finding a solution to this problem, one adopts either a high-coherence model or a low-coherence model. The second is usually referred to as the coupled-power model (1).

To this point, no assumption has been made regarding the relative coherence of the individual pulses at the output of the waveguide. However, to determine the net pulse shape at the output, one must decide whether to add the pulses coherently or incoherently. If one assumes that the pulses at the output are incoherent, the power at any instant in time is given by the sum of the power in the individual pulses. This low-coherence approach which is the basis for the coupled-power model, predicts that in the long-length regime the net output pulse will be Gaussian in shape and broadened relative to the input pulse by an amount

proportional to the square root of the waveguide length L and the differential group velocity ΔV of the two waveguide modes:

$$\sigma_t = \frac{1}{2\Delta V}\sqrt{(Ll_c)}, \quad L >> l_c \tag{2.6}$$

where σ_t is the root mean square (rms) broadening and l_c is the coupling length (5).

When the source coherence is high, the small pulses at the output of the waveguide interfere coherently. As a result, the shape of the net pulse depends on the relative phase of the constituent pulses and will be extremely different from Gaussian. In this situation the coupled-power model can predict only the average pulse shape at the output of a waveguide. It cannot predict the actual pulse shape that might be observed in a given waveguide, or how the pulse shape might change when the state of polarization or the wave-length of the source is changed.

2.4 **Principle State of Polarization**

In time domain, when pulse propagates along a long fiber, it has random mode coupling as the birefringence axes changes. The pulse splits at every axis change and thus become complicated. In frequency domain, the output SOP for different frequencies traces an irregular trajectory on Poincarè sphere.

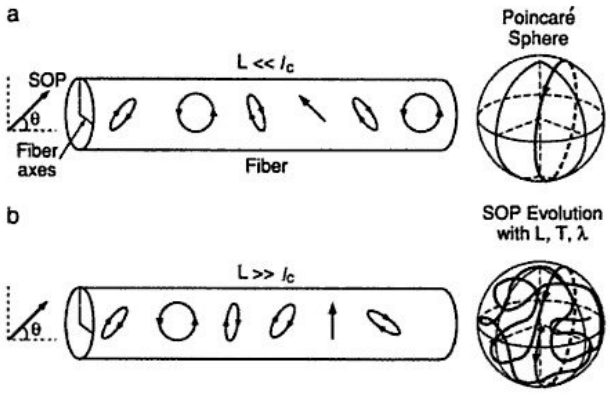

Figure 2.7 Output polarization evolution for (a) short and (b) long fibers under varying length, temperature or wavelength

In 1986, Poole and Wagner developed the Principle States Model for long fibers (6). It characterizes PMD both in time domain and frequency domain. In time domain, when people launch the signal of different SOP into the long fiber which has PMD much smaller than the pulse width and has no polarization dependent loss (PDL), there exist two orthogonal launch SOP so that the bit-error rate are minimum. In these two cases, the pulses are undistorted, and are the slowest and the fasted pulses of the entire different SOPs launched. These two SOP is called principle state of polarization (PSP). In frequency domain, input PSP is defined as the input SOP such that the output SOP is independent of frequency over a small span to the first order.

The corresponding output SOP is called output PSP. Without PDL in system, the input PSPs and output PSPs are two orthogonal pairs. The output PSP is related to the input PSP by the transmission matrix of the fiber. In Jones calculus, the relation is

$$E_{out}(\omega) = JE_{in}(\omega) \tag{2.7}$$

In stokes space, the relations is:

$$S_{out}(\omega) = R(\omega)S_{in}(\omega) \tag{2.8}$$

For ideal short fibers, the PSPs are just the birefringence axes (Fig.2.8 a). The output PSP is the same for all the frequency. For a fixed input SOP, the output SOPs for different frequencies are on a circle that is symmetric about the birefringent axis. Though for long fibers, with a fixed input SOP the output SOP for different frequencies traces an irregular trajectory rather than a circular on Poincarè sphere, but within a small frequency span centred at certain frequency, the SOP is approximately on an arc which is a part of the circle symmetric about the PSP for this certain frequency (1).

As shown in Fig. 2.8 (b) for a certain frequency ω_1 and a small span $\Delta\omega$, $SOP\left(\omega_1 - \frac{\Delta\omega}{2}\right)$ and $SOP\left(\omega_1 + \frac{\Delta\omega}{2}\right)$ are approximately on the circle symmetric about $PSP(\omega_1)$

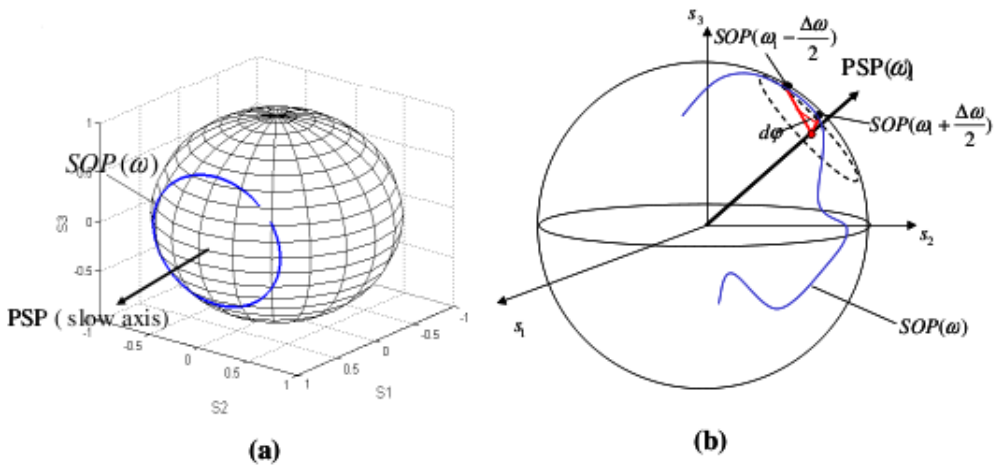

Figure 2.8 (a) output principle state of polarization for an ideal short fiber is the birefringent axis and is the same for all frequency. (b) output PSP of a certain frequency for a long fiber.

Assume that the angle of the arc between $SOP\left(\omega_1 - \frac{\Delta\omega}{2}\right)$ and $SOP\left(\omega_1 + \frac{\Delta\omega}{2}\right)$ is $d\varphi$, then the DGD between the two orthogonal PSP of frequency $d\omega_1$ is:

$$\tau(\omega) = \left|\frac{d\varphi}{d\omega}\right| \qquad 2.9$$

2.5 Higher order dispersion effects

The Principal States Model assumes that the optical loss in the fiber does not depend on polarization and that the coherence time of the source is greater than the PMD-induced time shift involved. This assumption is equivalent to assuming that the net time delay caused by PMD in the span is small compared with the bit period. But when the coherence time of the source became comparable to the differential delay time, we have higher order dispersion. This means that the differential delay time and the dispersion vector are themselves frequency dependent and may vary over the bandwidth of a source.

In the frequency domain, second-order dispersion manifests as a linear frequency dependence of the dispersion vector, and in the time domain its

manifest as a linear frequency dependence in the polarization vectors and in the delay items τ_+, τ_- of the output electric field formula:

$$E_2(t) = c_+\varepsilon_+ E_1(t+\tau_+) + c_-\varepsilon_- E_1(t+\tau_-) \qquad 2.10$$

where $E_1(t)$ is the time-varying input field, c_+ and c_- are the complex weighting coefficient, and ε_+ and ε_- are the unit vectors specifying the output polarization states of the two components.

The time domain effects, act as an effective chromatic dispersion that is opposite in sign for the two principal states (7; 8).

2.6 **Statistical treatment of PMD**

Modeling the PMD using a three-dimensional dispersion vector Ω, and allowing this vector to grow in a random-walk-like process along the fiber, we can demonstrate theoretically that the average delay time has a square root of length dependence (Fig. 2.8), and that the probability density function is Maxwellian (1) (Fig. 2.9).

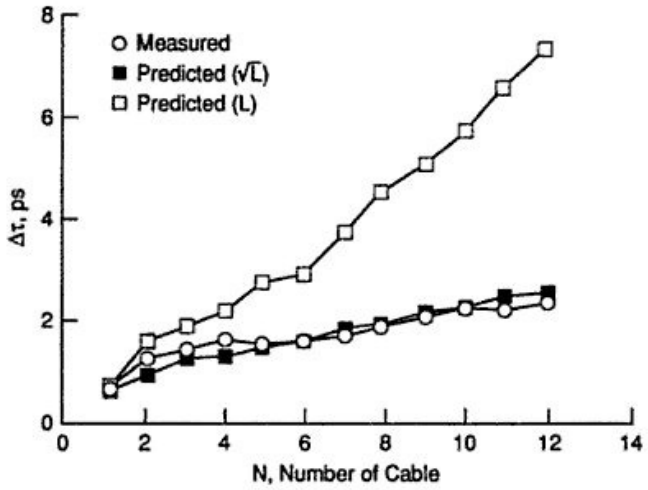

Figure 2.9 Length dependence of PMD in a concatenated cable span. (9)

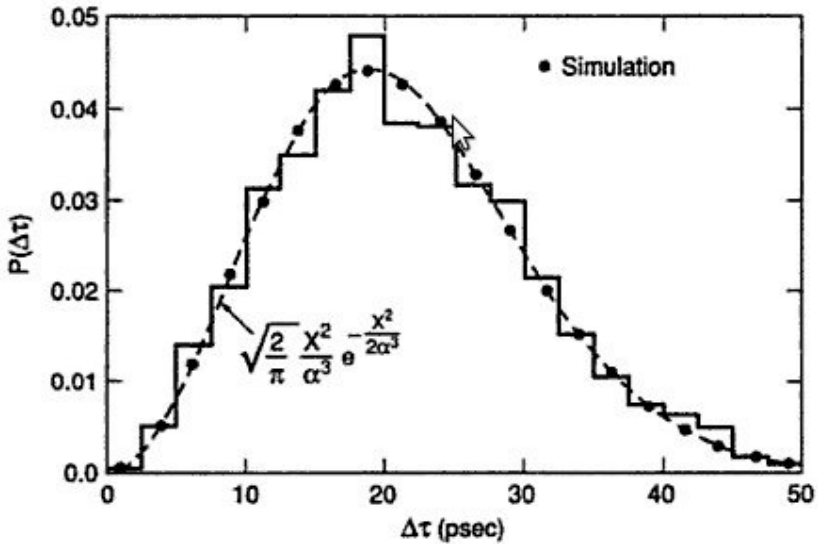

Figure 2.10 Measured distribution of differential delay times in 10 Km spooled fiber subjected to varying temperature. Dashed curve is a Maxwellian fit. (10)

Knowing that the polarization-dispersion vectors Ω provides a representation of PMD, and it could be related to the birefringence in a fiber through the vector equation

$$\frac{\partial \Omega}{\partial z} = \frac{\partial W}{\partial \omega} \oplus W X \Omega \qquad 2.11$$

(where z represent the position along the fiber, and W is a three-dimensional vector representing the local birefringence of the fiber), if the birefringence is treating as a stochastic process, the PMD of a long span could be related to the statistical properties of the local fiber birefringence (11).

For example, a fiber with uniform birefringence $\Delta\beta$ subjected to random perturbing birefringence, has mean square differential delay time between the principal states in the long-length regime given by:

$$\left\langle \Delta\tau^2 \right\rangle = \left(\frac{d\Delta\Delta}{d\omega} \right)^2 L l_c \; ; \qquad L >> l_c \qquad 2.12$$

where L is the fiber length and l_c ,is the correlation length defined previously.

The frequency derivative of the birefringence in Eq. (2.10) is just the intrinsic PMD of the fiber.

Comparison of Eq. (2.10) and (2.4) shows that the principal states model and the coupled-power model results are related through a simple numeric constant:

$$\left\langle \Delta\tau^2 \right\rangle = 4\sigma_t^2 ; \quad L >> l_c \tag{2.13}$$

As noted previously, the correlation length l_c in Eq. (2.10) is highly sensitive to mechanical stresses induced by spooling or cabling fiber. Because of the dependence of PMD on the correlation length, PMD is also dependent on such perturbations. As a result, a single timer may show varying levels of PMD depending on whether it is spooled or cabled. Recent measurements indicate that cabling may tend to increase l_c, and, thus, PMD levels by reducing the mechanical stresses relative to those on the spool.

2.7 PMD POWER PENALTIES AND PMD LIMITS

As we have already said, PMD is a time-varying stochastic effects, so also the system penalties are time-varying. It can be seen in the figure 2.6.1 where is plotted the variation of the bit error rate during a day, from the sunrise to the sunset.

This is an experimental demonstration of PMD induced variation in bit error rate performance in a digital lightway system.

Under this observation, a system designed with adequate margins for normal conditions, can have unacceptable penalties under condition of extremely high PMD. To obtain an estimation of the limitation imposed by PMD is assumed that the pulse bifurcation is the dominant mechanism for pulse broadening (as described in Eq. 2.10) the power penalty for a NRZ digital system is:

$$\varepsilon(dB) \approx A\frac{\Delta\tau^2\gamma(1-\gamma)}{T^2} \tag{2.14}$$

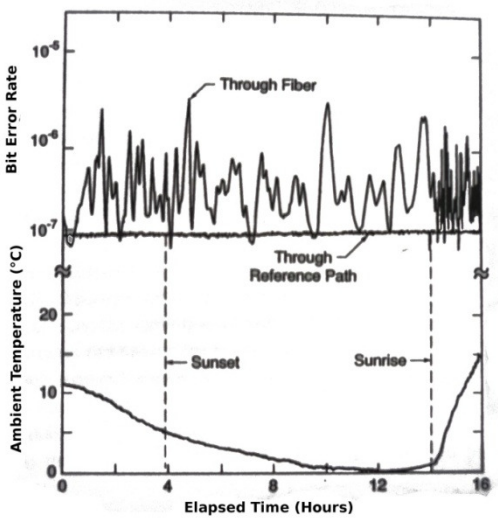

Figure 2.11 Bit error Fluctuations in a digital system caused by PMD and changing ambient temperature. (12)

where A is a dimensionless parameter that depends on the optical pulse shape receiver filter characteristic (table 2.6.1 shows some value of A for several pulse shapes) , T is the full width at half maximum of the optical pulse, and γ (that vary between 0 and 1) is the power-splitting ratio between the two components.

This equation shows that the system penalty has a quadratic dependence on both the differential delay time and bit rate. The penalty goes to zero only when γ is 0 or 1, specifically in the case where all the power is in one of the component pulses.

Pulse Shape	A
Gaussian	25
Raised cosine	22
Square	12
25% rise-fall	15
Triangular	24

Table 2.1 Values for Various pulse shape

As said before the power penalty caused by PMD will vary in a random way, owing to the random variation of the parameters γ and $\Delta\tau$, so for the purpose to establish a PMD limit, its stipulated that penalties in excess of 1 dB are

unacceptable; and that the allowable probability for such outage is less than 1 in 18'000. This probability correspond to 4σ on a Gaussian distribution, and in term of cumulative outage time this probability correspond to 30 minutes per year.

The probability of observing a penalty greater than 1 dB is determined by the probability density function for ε. Assuming a Maxwellian distribution for $\Delta\tau$ and a uniform distribution of γ, and statistical dependence for the two parameters, the Eq. (2.12) leads to a simple exponential probability density function for the power penalty:

$$P(\varepsilon) = \eta e^{(-\eta\varepsilon)} \qquad 2.15$$

Where $$\eta = {16T^2}/{A\pi\langle\Delta\tau\rangle^2} \qquad 2.16$$

and $\langle\Delta\tau\rangle$ denotes the average differential delay.

The probability of observing a penalty greater than 1 dB is obtained by integrating the above equation (2.13) from 1 to infinity:

$$Prob\{\varepsilon \geq 1\} = \int \eta e^{(-\eta\varepsilon)} = e^{-\eta} \qquad 2.17$$

In Fig. 2.12 its shown the distribution of power penalties obtained in a computer simulation of a digital system in which fiber PMD is modeled by a concatenation of 1000 uniformly birefringent fiber sections having randomly oriented fiber axes. Chirp-free Gaussian pulses were sent through PMD and detected by a receiver with a fourth-order Bessel shape filter characteristic. The points in the figure show the logarithmic of frequency of occurred penalties in10'000 simulated fibers. The solid curve demonstrates the expected dependence according to the Eq. (2.13).

Because the model used for PMD included all higher order dispersion effects, the agreement between the data in Fig. 2.12 and Eq.(2.13) demonstrate the validity of assuming that first-order effects are the dominant source of pulse broadening under small penalty conditions.

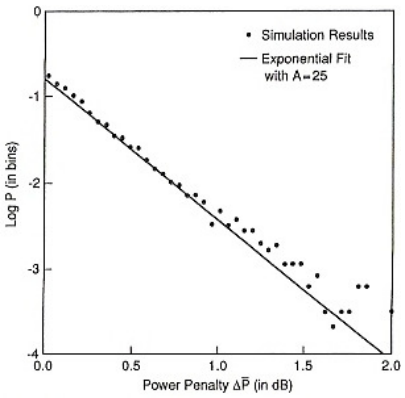

Figure 2.12 Distribution of power penalties and exponential fit for a simulated digital system containing PMD

To obtain a PMD limit, the left-hand side of the Eq. (2.15) is set equal to the allowable probability of 1 in 18'000 that correspond to the outage time of 30 minutes per year.

This leads to the condition $\eta = 9.8$, or assuming Gaussian pulse shape with $A = 25$:

$$\left.\frac{\langle \Delta\tau \rangle}{T}\right|_{limit} = \mathbf{0.14} \qquad 2.18$$

This equation indicates that for a digital system to avoid incurring a power penalty greater of 1 dB for a fractional time of 30 minutes per year, the average differential time between the principal states must be less than th 14% of the bit period.

To generate a bit-rate limit curve using the previous equation, we make use of the length- normalized parameter $PMD = \langle \Delta\tau \rangle / \sqrt{L}$ a and the bit rate $B = 1/T$ so that equation becomes: .

$$B^2 L = \frac{0.020}{(PMD)^2} \qquad 2.19$$

In Fig. 2.13 is shown the plot of PMD limit corresponding to the previous formula Eq. 2.19 for an example system of 100km long span. This system should have a PMD of less than $1.4\,ps/\sqrt{km}$ to operate with a bit rate of 10 Gb/s. But this limit is

not a hard limit, because a system operating at the PMD limit would operate normally for the majority of time; it's only during the outage events that the system would experienced significant performance degradation.

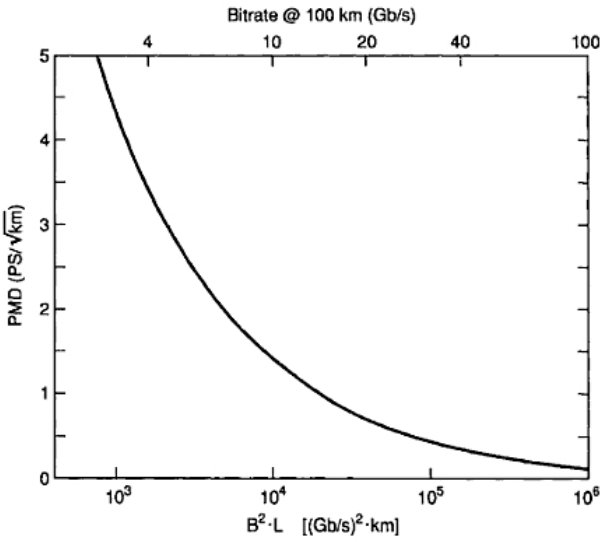

Figure 2.13 PMD limit for a digital system

2.8 Jones vector and stokes vector

As the light beam propagates in the z direction, the electric field, which lies in the *x-y* plane, can be viewed as the superposition of two orthogonal linearly polarized fields: *x* and *y* components.

As the light beam propagates in the z direction, the electric field, which lies in the *x-y* plane, can be viewed as the superposition of two orthogonal linearly polarized fields: *x* and *y* components.

In time domain, for any point in space, the electric field is:

$$\vec{\varepsilon}(t) = \vec{a}_x E_{x0}\cos(\omega t + \varphi_x) + \vec{a}_y E_{y0}\cos(\omega t + \varphi_y) \qquad 2.20$$

In the previous equation, E_{x0} and E_{y0} are the amplitudes of the x and y component respectively, while φ_x and φ_y are the phase of these two

components. We can see that the electric field varies with time, but the variations are different due to the difference in amplitudes and phases of the components.

We use State of Polarization (SOP) to name this variation. In the case $\varphi_x = \varphi_y$, the field direction, which is determined by the ratio of E_{x0} and E_{y0}, is constant, and we get linear polarization.

In the case $\varphi_x \neq \varphi_y$, we get elliptical polarization, which means that the end of the electric field vector evolves on an ellipse in the x-y plane with time. If $\varphi_x > \varphi_y$, the ellipse is left-handed, which means the evolution is counter-clocked wise, while if $\varphi_x < \varphi_y$, the ellipse is right-handed, which means the evolution is clock wise. (We always assume that the observer looks towards the propagation direction of the light.).

Conditions	$\varphi_x = \varphi_y$	$\varphi_x > \varphi_y$	$\varphi_x < \varphi_y$
SOP	linear polarization, $\tan\theta = \frac{E_{y0}}{E_{x0}}$ (θ is the field direction from +x axis)	Left-handed elliptical polarization.	Right-handed elliptical polarization.
		If $\varphi_x = \varphi_y + \frac{\pi}{2}$ and $E_{x0} = E_{y0}$, left-hand circular (LCH)	If $\varphi_y = \varphi_x + \frac{\pi}{2}$ and $E_{x0} = E_{y0}$, right-hand circular (RCH)

Table 2.2 SOPs in different cases

Jones calculus is a simple and clear way to describe SOP and the media where the light propagate and its SOP evolves. Jones calculus includes *1×2* Jones vectors which describe the SOP, and *2×2* Jones matrices which describe the media. In Jones calculus, the electric field of a certain SOP is written as:

$$E = \begin{bmatrix} E_x \\ E_y \end{bmatrix} = \begin{bmatrix} E_{x0} e^{j\varphi_x} \\ E_{y0} e^{j\varphi_y} \end{bmatrix} \qquad 2.21$$

If we normalize the Jones vector, all the SOP can be written as:

$$\begin{bmatrix} \cos\theta \\ \sin\theta x e^{j(\varphi_y - \varphi_x)} \end{bmatrix} \quad 2.22$$

The normalized Jones vector for horizontally and vertically linear polarization and the right-hand and left-hand circular polarization are:

$$\begin{bmatrix} 1 \\ 0 \end{bmatrix}; \begin{bmatrix} 0 \\ 1 \end{bmatrix}; \frac{1}{\sqrt{2}} \begin{bmatrix} 1 \\ j \end{bmatrix}; \frac{1}{\sqrt{2}} \begin{bmatrix} 1 \\ -j \end{bmatrix} \quad 2.23$$

If the two SOPs E_1 and E_2 are orthogonal, this means these two Jones vector satisfies: $Dot(E_1, E_2) = 0$, where E_2 is the conjugate of E_2 .

Obviously, Horizontal linear polarization and vertical linear polarization, *RHC* and *LHC* are two orthogonal pairs. Any SOP can be decomposed to the combination of two orthogonal SOP pairs. When the light propagate in a media, its SOP evolves. We use Jones matrix to describe how this media changes the input SOP into the output SOP.

The relationship is :

$$\begin{bmatrix} E_{x_{out}} \\ E_{y_{out}} \end{bmatrix} = \begin{bmatrix} J_{11} J_{12} \\ J_{21} J_{22} \end{bmatrix} \begin{bmatrix} E_x \\ E_y \end{bmatrix} \quad 2.24$$

where $J = \begin{bmatrix} J_{11} J_{12} \\ J_{21} J_{22} \end{bmatrix}$ is Jones Matrix. For example, here we introduce two simple but frequently used Jones matrix. One is for the retarder (or wave-plate) which has the fast axis at x axis:

$$R(\varphi) = \begin{bmatrix} e^{j\frac{\varphi}{2}} & 0 \\ 0 & e^{j\frac{\varphi}{2}} \end{bmatrix} \quad 2.25$$

it retard the phase of y field component by φ . The other one is for rotating the coordinates by angle θ relative to the $+x$ axis:

$$S(\varphi)=\begin{bmatrix}\cos\theta\sin\theta\\-\sin\theta\cos\theta\end{bmatrix} \quad 2.26$$

For a complicated or composite optical device, to get its Jones matrix, we can just multiply the Jones matrix of the simple operations or the individual elements in order. In a system with no loss, the Jones matrix can be simply expressed as the products of the Jones matrix for retarders and axis rotations.

Similar to Jones calculus, stokes vector and Müller matrix in stokes space is another way to describe SOP and the media. Stokes parameters (s0 , s1 , s 2 , s3) are measurable parameters:

$$s_0 = I_0 + I_{90} = I_{45} + I_{135} = I_{RCH} + I_{LCH} = E_{x0}^2 + E_{yo}^2 \quad 2.27$$

$$s_1 = I_0 - I_{90} = E_{x0}^2 - E_{y0}^2 \quad 2.28$$

$$s_2 = I_{45} - I_{135} = 2E_{x0}E_{y0}\cos(\varphi_y - \varphi_x) \quad 2.29$$

$$s_3 = I_{RCH} - I_{LCH} = 2E_{x0}E_{y0}\sin(\varphi_y - \varphi_x) \quad 2.30$$

where I_0 is the intensity of the horizontal component, and the meaning of I_{90} , I_{45} , I_{135} , I_{RHC} and I_{LHC} are similar. The stokes vector is the normalization of the vector (s_1, s_2, s_3). This vector is always plotted on the unit sphere known as Poincarè sphere in 3-D space. By this tool, SOP can be visualized and conveniently analyzed.

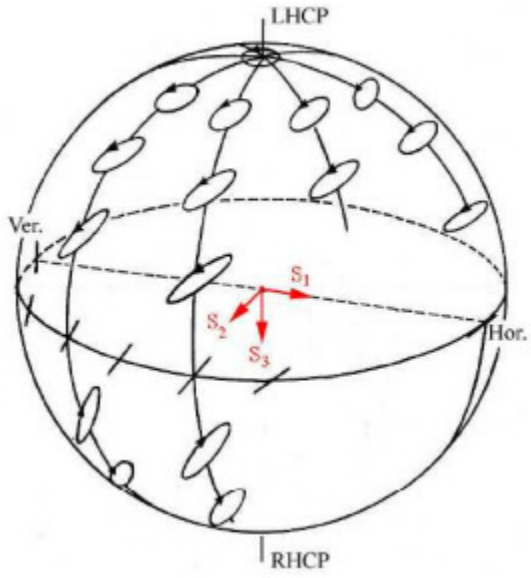

Figure 2.14 Pintcarrè Sphere

The table below shows the stokes vector for some special SOPs:

(s_1, s_2, s_3)	**SOP**
$(1,0,0)$	Horizontal linear polarization
$(-1,0,0)$	Vertical linear polarization
$(0,1,0)$	45 degree linear polarization
$(0,-1,0)$	135 degree linear polarization
$(0,0,1)$	Right-hand circular polarization
$(0,0,-1)$	Left-hand circular polarization
$s_3 = 0$	Linear polarization
$s_3 < 0$	Right-hand elliptical polarization
$s_3 > 0$	Left-hand elliptical polarization

Table 2.3 Stokes vector for different SOPs

On the Poincarè sphere, all the linear polarizations lie on the equator. The north pole and the south pole are LHC and RHC respectively. SOPs are left-hand elliptical on the north of the sphere, and right-hand elliptical on the south. Every pair of orthogonal SOPs are the two points symmetric about the center of the sphere.

In stokes space, a 3 × 3 matrix called Müller matrix describe the media's effect on the SOP evolution.

Jones calculus and the stokes vector have their own advantage comparing to each other. Jones vector and matrix are smaller in size, and they describe the field directly. However, Jones vector can only describe polarized light, while stokes vector can also describe partially polarized light and unpolarized light. Moreover, visualization is also an advantage of stokes space.

CHAPTER 3
PMD MITIGATION

3.1 Introduction

As explained in the previous chapter, PMD can cause several undesirable effects that could be obstacles to high speed telecommunication through optical fibers. Such effects are not limited to digital communication systems but affect analog communication systems as well.

With the evolution of specialized manufacturing methods, PMD in present day, telecommunication grade fibers is kept very low (< 0.1ps/√km). Still, no matter how good the fiber may be, at some bit-rate-length product, PMD will be an issue. Hence, there is need to investigate strategies for PMD mitigation.
Over the years, research groups from around the globe have proposed and/or demonstrated different strategies for PMD compensation. In this chapter an overview of these strategies shall be given. Their relative merits and demerits will also be mentioned. Following that, methods to increase the tolerance of a fiber-optic communication system to PMD, will also be discussed.

3.2 PMD compensation strategies

The more widely researched PMD compensation techniques are summarized in the next section, followed by a summary of other techniques.

3.2.1 Optical PMD compensation techniques

Optical PMD compensators (Fig. 3.1) typically comprise of a polarization controlling device, an optical delay element (fixed or variable) and allied

electronics which provide control signals to the optical components based on feed-back information about the link's PMD.

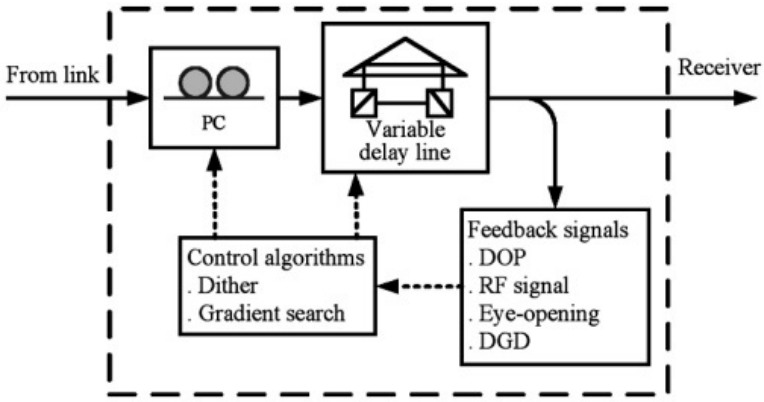

Figure 3.1 Structure of an optical PMD compensator

3.2.2 Classification based on PMD monitoring techniques

PMD is a randomly changing entity. Adaptive techniques are necessary to continually track the changing DGD and PSPs and perform effective PMD compensation. It is also necessary to provide reliable estimates of the DGD and PSPs to the PMD compensator. The control signals to the variable delay element and the polarization controller can be generated using different PMD monitoring techniques. A summary of the monitoring techniques used in feed-back based, optical PMD compensation systems is given below.

One of the earliest techniques used for monitoring PMD is the observation of the power levels of specific tones in the received ***RF spectrum*** of the base-band signal (13). The monitor signal, based on which a control signal to the polarization controller is generated, is proportional to the expression:

$$1 - 4\gamma(1-\gamma)\sin^2(\pi f \Delta\tau) \qquad 3.1$$

where, γ is the ratio of power-splitting between the two input PSPs, fc is the center frequency of the band-pass filter for extracting the monitor signal and Δt is the net DGD, from the start of the link up to and including the delay element used

in the compensator (13). The principle behind this technique is the following. PMD causes reduction of power in the main lobe of the received baseband spectrum. Therefore, the amount of PMD to be compensated for can be estimated by measuring the power level of the received baseband spectrum. The power level of a single tone (corresponding to half the bit-rate), that can give an unambiguous estimate of PMD, has been used as the monitor signal in (13). The band-pass filter is used to extract the monitor signal from the baseband spectrum. The adjustments to the compensator are made with the goal of maximizing the monitor signal, which would happen when PMD effects are effectively nullified.

One drawback of using the above described technique is that the required hardware is bit-rate dependent. The photo-detector, band-pass filter, RF amplifiers etc can be used for one data rate only.

Another recently developed PMD monitoring technique is based on the ***degree of polarization (DOP)*** of the received optical signal. PMD can depolarize the optical signal. This in turn reduces the DOP (since DOP is a measure of the amount of optical power that is in the polarized state). The reasons for reduction in DOP due to PMD effects in digital communication systems have been identified and described in (14) and (15).

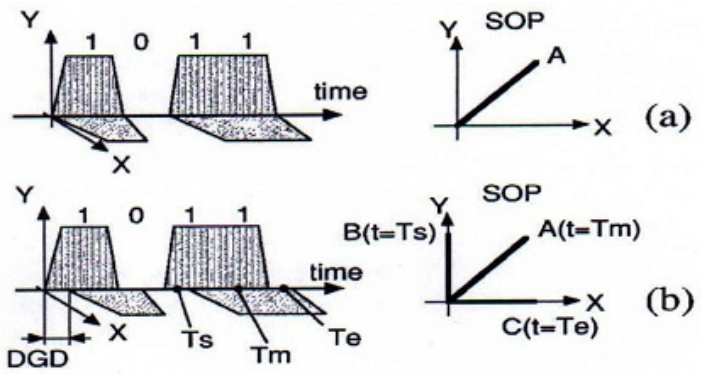

Figure 3.2 Depolarization in digital optical signals due to pmd. Comparison of cases (a) without pmd and (b) with pmd

Figure 3.2 illustrates the role of PMD in causing depolarization in digital optical signals. The merits of using DOP evaluation in the PMD monitoring mechanism are several in number. DOP is bit-rate independent and largely modulation format independent. To a good extent, techniques based on DOP evaluation reduce hardware complexity. On the other hand, since DOP is also affected by amplified spontaneous emission (ASE) noise and non-linear effects, it's sensitivity to PMD may get reduced in long distance fiber-optic links.

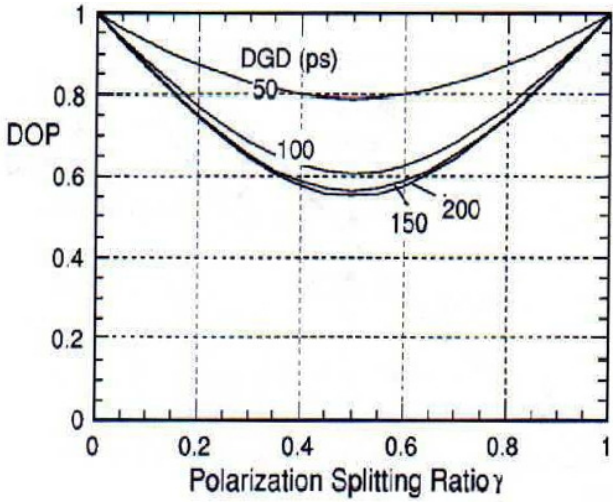

Figure 3.3 Simulated DOP versus γ, the power splitting ratio between the two input PSPs of a PMD device, for a 10-Gb/s, lithium niobate-Mach-Zehnder, NRZ (non-return to zero) modulation, for different DGD values

Figure 3.3 is a plot showing the sensitivity of DOP to DGD. It is significant for more than one reason. Firstly, it confirms that DOP can be a good indicator of PMD. Also, it shows that the sensitivity of DOP to DGD is greatest when the power splitting ratio, γ, is 0.5.

Another monitoring technique is based on inter-symbol interference caused by PMD in digital fiber optic systems. The received eye diagram is monitored and a control signal based on the amount of eye opening is generated.
For example, this technique should uses an integrated SiGe circuit, consisting of two decision circuits, as the eye monitor (16). The correlation between the bit error rate (BER) and the signal generated by the ***eye monitor*** has been reported

to be good. The goal of PMD compensation in digital systems is the minimization of BER. However, the BER by itself cannot be directly used as a quantity representative of PMD, because it cannot be measured with high accuracy in a short period of time. Methods such as the *eye monitor technique* help to overcome such difficulties by providing a control signal which is correlated to the BER.

In principle, eye opening monitoring enables the most precise feedback signal, but it requires high-speed electronics

3.2.2.1 Classification based on order of compensation

Depending on the versatility and compensation capability, PMD compensators can be classified as half-order, first-order and second-order compensators.

A ***half-order compensator*** comprises of a polarization controller and a fixed optical delay element. In addition, there is a feed-back control mechanism to provide appropriate control signals to the polarization controller. The principle of operation is that the polarization controller is adjusted so as to minimize the combined DGD of the link and the compensator. The delay element is fixed. Since this compensator can only compensate for a fixed amount of DGD, rather than varying delays, it is sometimes referred to as a half-order compensator. A half-order compensator configuration, consisting of a polarization controller and a segment of high-birefringence fiber (fixed delay element) has been described in (13).

The polarization controller adjustment was made based on a feed-back signal which was the power level of the tone corresponding to half the data rate in the received base-band spectrum. Figure 3.4 is a reproduction of the PMD compensator configuration described in (13).

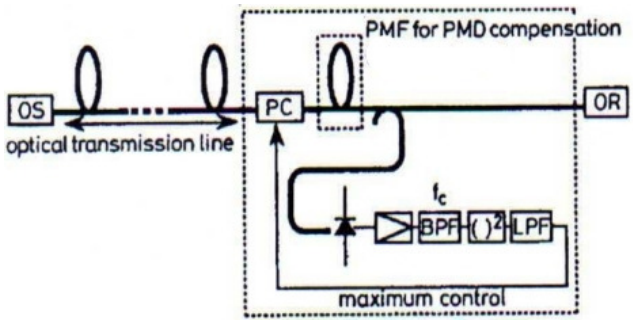

Figure 3.4 Half-order PMD compensator. (OS: optical source, PC: polarization controller, LPF and BPF :low-pass and band-pass filters, ( )2: square-law detector, OR: optical receiver)

A ***first-order PMD compensator*** is slightly more complex than a half-order compensator since it has a variable delay element instead of a fixed delay element. A feedback mechanism provides control signals for adjusting both the polarization controller and the delay element. The first-order compensator can be employed to counter different amounts of DGD values.

The first-order configuration described in (17) uses a polarization controller and a variable delay element. Based on the feedback signal (which is similar to the one adopted in (13)), polarization and delay adjustments are executed so as to minimize the PMD effects. In order to increase the accuracy of the PMD compensation, the SOP of the optical signal may be scrambled before the signal is launched into the fiber link. Figure 3.5 is a block diagram of the PMD compensation system described in (17).

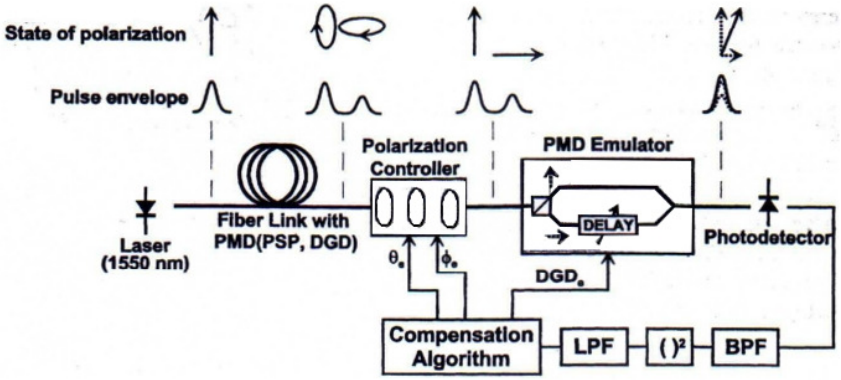

Figure 3.5 First-order adaptive PMD compensator functional block diagram. (LPF and BPF: low-pass and band-pass Filters, ( )^2: square-law Detector)

Another approach for first-order PMD compensation is called the PSP transmission method. It was first described in (18). The PSP transmission method is a pre-compensation method in which a polarization controller is used to align the SOP of the optical signal with a PSP of the fiber link. Figure 3.6 (19) shows the block diagram of a first-order PMD compensator based on the PSP transmission method.

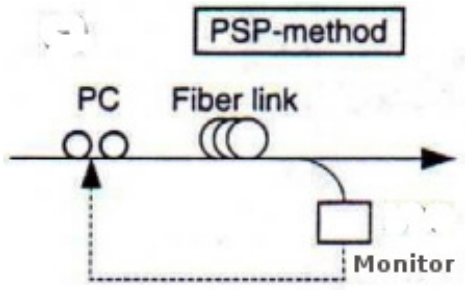

Figure 3.6 First-order PMD compensation with PSP method

Given the increasing data-rates and the expanding bandwidth, importance has been attached to *second-order PMD compensation* also. One proposed configuration uses two polarization controllers and two pieces of high-birefringence fiber . The compensator's PSPs are made to vary linearly with frequency so as to compensate for PMD over a larger bandwidth. The principle of changing the PSPs of the compensator as a linear function of frequency is made use of in the configuration described in (20) also. However, the set-up adopted in (20) includes three polarization controllers and two variable delay lines (or one variable delay line and one Faraday rotator). Figure 3.7 is a block diagram of the compensator described in (21).

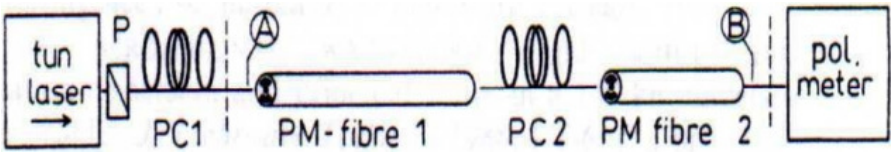

Figure 3.7 Second-order PMD compensator block diagram. (PC1 and PC2: polarization controllers)

3.2.3 Electrical PMD Compensation

The first demonstration of PMD compensation was made by equalizing the electrical signal before the receiver with a Electronic distortion equalizers (EDEs). Many variations of this idea have been proposed, including opto-electrical compensator that are based on polarization diversity detection, so that two or several electrical signals can be combined to yield a compensated signal. More recent approaches have focused on various kinds of prediction schemes and references therein.

In general, however, electrical schemes are robust and will improve the signal against all kinds of transmission impairments; and thanks to their integration as a simple electronic chip into an optical receiver board, they offer a promising and potentially low-cost alternative or complementary approach to adjustable optical means for reach and bit-rate upgrade .

On the drawback side is that they do not perform as good as optical PMD compensator due to the loss of optical phase and polarization information after detection by a photo-diode.

Nevertheless, a single, low- cost EDE chip implemented in each receiver will potentially enable progress toward extended reach lengths, or toward higher bit rates. Moreover, it relaxes the design constraints on the optical infrastructure. In certain cases it can allow the removal of expensive, finely tuned optical distortion compensator inserted at the receiver side (22).

Two different basic types of electronic equalizers exist, using either analog or digital processing means (fig. 3.8). Both equalizer types can be realized as an application-specific integrated circuit (ASIC), on a chip area of a few square millimeters, and adapt automatically to any slowly varying distortion without the need for a training sequence.

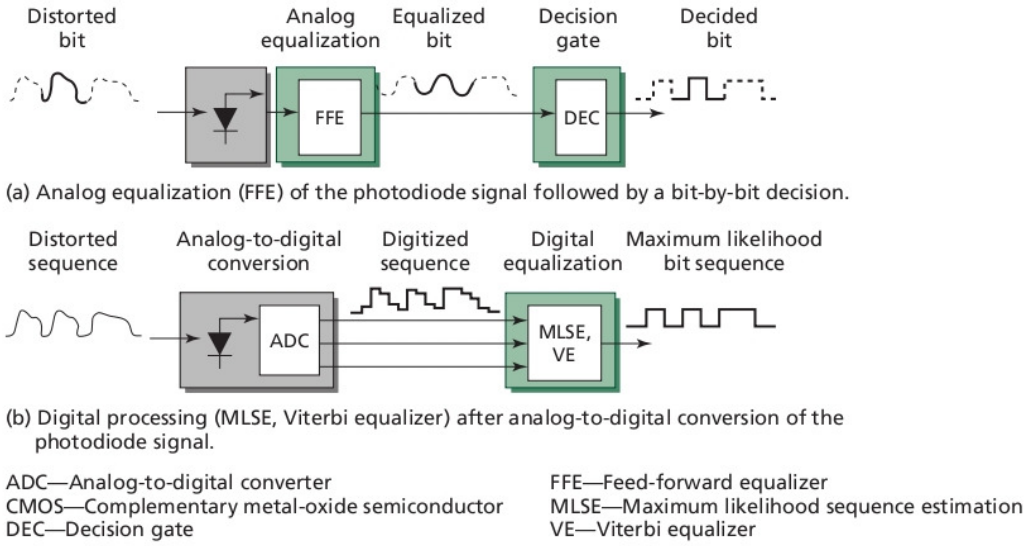

Figure 3.8 Analog and digital electronic distortion equalizers.

Analog electronic equalizers include multi-tap feed-forward equalizers (FFE), decision feedback equalizers (DFE), and combinations of both. The DFE includes the decision gate. This type of equalizer processes several consecutive bits at the same time, but the data then will be decided bit-by-bit.

Different techniques are available for the automatic adaptation of analog electronic equalizers. In systems using FEC, the count of the corrected errors can be used as the feedback signal for the adaptation algorithm. The error count is applied in a dither algorithm for adaptation of the FFE and the decision circuit, where each tap and the decision threshold, respectively, are optimized independently to minimize the error count. Due to the random occurrence of bit errors, a sufficiently high number of errors must be evaluated in order to obtain a stable feedback signal.

An alternative method (23) is to insert an eye monitor in parallel with the decision circuit. This eye monitor evaluates the vertical eye opening of the received data signal by measuring the mean and rms values of ones and zeros. Two versions are possible:

- The serial eye monitor consists of a decision circuit, where the threshold and sampling phase are continuously tuned.

- The parallel eye monitor uses an analog-to-digital converter (ADC).

Both eye monitors provide a parameter that is related to the eye opening or the Q-factor of the eye diagram of the equalized signal. This parameter is then used in the same dither algorithm as with the error count feedback. Since the eye monitor works independently of the decision circuit, it enables a faster adaptation speed than obtained by using the FEC error count.

Digital electronic equalizers use the maximum likelihood sequence estimation (MLSE) by implementation of the Viterbi algorithm (22). They require more complex signal processing compared with the analog equalizer. First, it converts the received data signal into digitized samples using an analog-to-digital converter with 3–4 bit resolution. Then it calculates the most probable received sequence in a digital processor using the Viterbi algorithm: i.e., it simultaneously processes and decides a data sequence resulting in a potentially higher performance compared to the analog type. The adaptation of the digital equalizer is done by a statistical analysis of the formerly received data signals, which are available within the digital equalizer. The adaptation speed is then comparable to that of the analog equalizer using the parallel eye monitor.

3.3 Increasing PMD tolerance in a fiber-optic system

In addition to compensating for PMD, there are methods by which a fiber optic communication system's tolerance to PMD can be enhanced. A well researched such method is the use of PMD resistant modulation formats. Forward-error correction (FEC) coding is another example. FEC can help increase the tolerance of a system to effects of noise, chromatic dispersion and PMD. An experiment described in (23) uses Reed-Solomon error-correcting codes along with a first-order PMD compensator to effectively increase the PMD tolerance of a 10-Gb/s system.

3.3.1 Modulation formats resistant to PMD effects

The most widely adopted signaling format in contemporary fiber optic communication systems is the NRZ (non return-to-zero). However, in recent years, novel modulation formats and their resistance to signal degrading phenomena, such as PMD, have also been studied widely.

Return-to-zero (RZ) signals are considered more resistant to penalties caused by broadening than NRZ. The reason for the increased resistance of RZ can be explained as follows (1). In the case of RZ modulation, the signal energy is more confined to the centre of each bit duration. As DGD increases, the power in isolated zeros rises only slowly. Whereas in the case of NRZ, this power rises quickly and combines with the ones to cause greater penalty (1). In addition to RZ, there are the chirped RZ (CRZ), classical solitons and dispersion-managed solitons (DMS). which are known to be more resistant to PMD effects. Classical solitons and DMS are considered more resistant to birefringence induced break-up. Just as dispersion and non-linearity balance each other to prevent pulse broadening, the non-linear attraction between the two polarization components prevents the break-up of a soliton or DMS pulse due to birefringence.

A comparison of the penalties incurred by NRZ, RZ, CRZ and DMS signals in the presence of high PMD, in a 10-Gb/s terrestrial system, has been made using computer simulation (24). The results showed that RZ, DMS and CRZ signals performed better than NRZ for spans of up to about 600 km. For longer spans, CRZ provided the best system performance. Examples of other modulation formats that have been studied and that are known to be more resistant to PMD than NRZ are, the phase-shaped binary transmission format (PSBT) (25) and optical duo-binary modulation which has been reported to be more resistant to higher order PMD effects also (26).

3.4 **Simulation's Compensator**

The structure of the compensator used in this study is shown below.

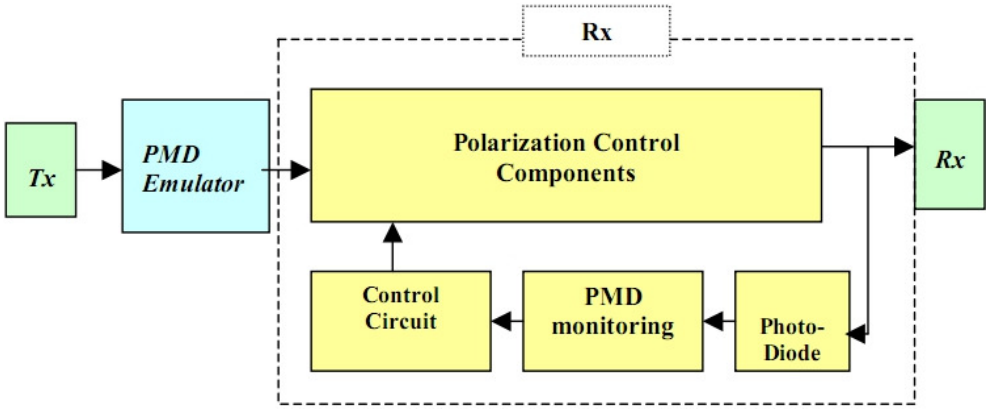

Figure 3.9 Block diagram of transmission link including the PMD compensator

The transmission is made through a NRZ modulator, @1553 nm in the third windows; and the power-splitting is set to 0.5, in order to obtain the worst waveform distortion.

At the compensator side (Fig.3.10) there is a polarization angle rotator, that rotates SOP of the incoming light, in front of a variable delay line; by rotating the SOP of the incoming lightwave it's possible to controls which component of the light is to be delayed.
In this setup the monitor is made through an eye opening monitor used as a feedback signal, but there isn't a control algorithm, that is made handily, by setting the better combination of SOP and delay, to controls the polarization rotator and the delay line.

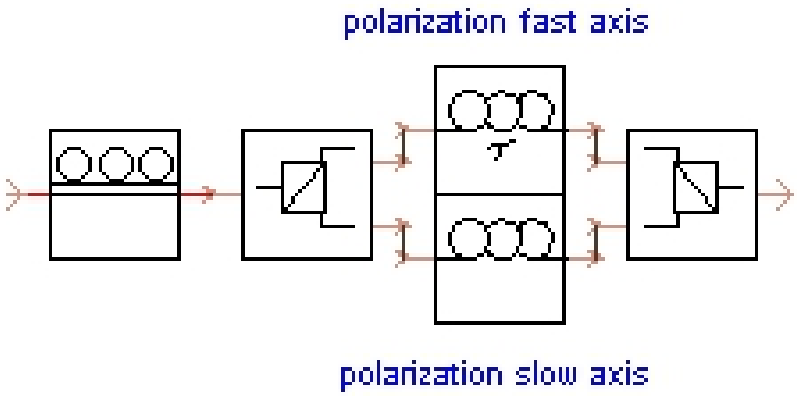

Figure 3.10 PMD Compensator Scheme

The compensator is composed by:

- 3 stage controller
- polarization beam splitter
- delay compensator
- polarization beam combiner

The ***3-plate polarization controller*** (28) is a polarization transformer, implemented as a hierarchical structure. It consists a half waveplate between two quarter waveplates, as shown in Figure 3.11 .

All of the waveplates are endlessly rotatable, but the two quarter waveplates have a fixed angular offset of 90°. This offset reduces the number of control variables, while still providing access to all polarization states. Although any angle can be entered for *Control1*, its functional range is from 0° to 360°. Similarly, the functional range for *Control2* is from 0° to 90°. As shown in Fig. 3.11, Control1 rotates all of the waveplates, while *Control2* provides an additional rotation to the half waveplate. The mapping of the two control angles to specific polarization changes is complex. Generally, values of *Control2* near 0° and 90° give small changes in ellipticity, while values near 45° give large changes. *Control2* also determines the range of azimuths that can be reached. On the other hand, values of *Control1* near 90° and 270° give large changes in azimuth,

while values near 0°, 180° and 360° give smaller changes. *Control1* also determines the range of ellipticities that can be reached. In this case the ellipticity was set to 0 in the PMD emulation, so C*ontrol2* is always set to 0, and only *Control1* varies in order to change the SOP of the incoming lightwave.

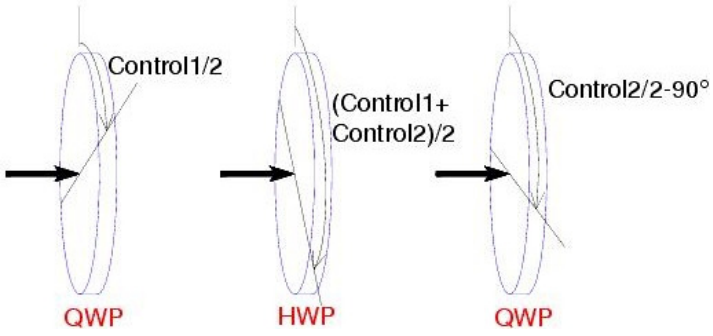

Figure 3.11 Polarization controller

The ***polarization beam splitter*** module simulates an ideal polarization beam splitter that divides the two polarization equally.

The operation of the polarization beam splitter is explained in Fig. 3.12. It can be considered to consist of two ideal linear polarizers oriented orthogonal to each other. The polarization components of the input optical signal, corresponding to the x- and y- axis of the device, are output at the ports OutputX and OutputY.

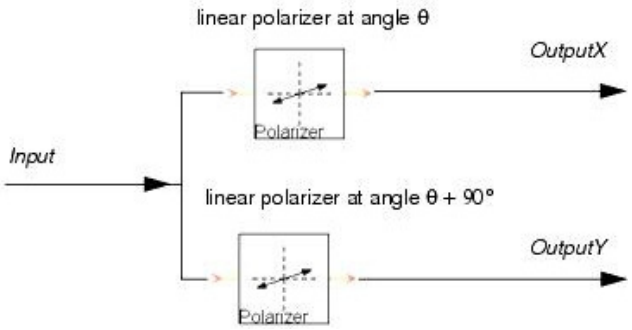

Figure 3.12 PBS Scheme

The ***delay compensator*** module imposes a variable time delay on an optical input signal. The original signal after that is splitted into the two polarization

mode, come to this device, where the fast axis is delayed, while the slow axis remains unalterated.

The ***polarization beam combiner*** (fig. 3.13) consists of two ideal linear polarizers at the input ports inputX and inputY, which are oriented orthogonally to each other. The polarizers are used to select the appropriate polarization components of each input signal and are followed by an ideal multiplexer, which adds the selected polarization components.

After the multiplexer, the signal is given to the input of the Signal-Converter module. When one Parameterized Signal is at the *inputX* port and another one with the same frequency is at the *inputY* port, the output spectrum of the multiplexer contains two signals with equal frequencies.

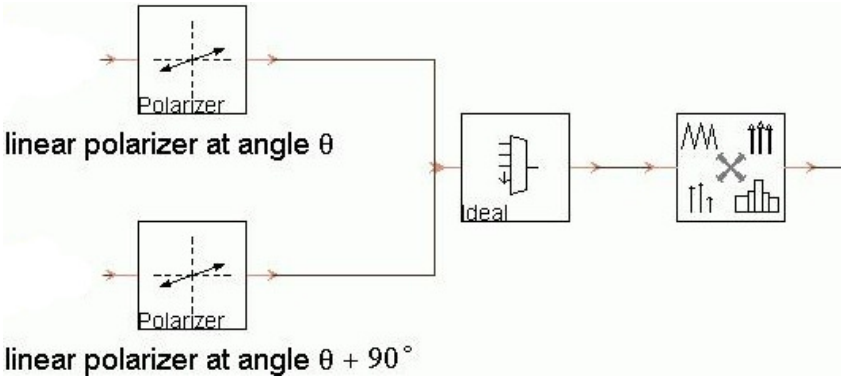

Figure 3.13 PBC Scheme

CHAPTER 4
PERFORMANCE LIMITATION DUE TO PMD

In this chapter is studied how the Polarization Mode Dispersion influences the performance of an optical communication systems, in a single or multi span system.

4.1 Introduction

Polarization Mode Dispersion, or PMD for short, is an important linear phenomenon occurring inside optical fibers that affects the performance of modern fiber-optic communication systems adversely. For a given fiber, PMD is supposed to be fixed. However, this is not the case in real communication systems because environment fluctuations cause PMD to vary randomly in time, which makes it difficult to compensate for PMD. Therefore, it is important to understand the statistical properties of pulse propagation induced by PMD. While the phenomenon of Polarization Mode Dispersion (PMD) has been known for years, it has only been recently that it has posed a serious, realistic problem for optical networks. PMD's negative effects result in a limitation of a networks bandwidth or length that is, of course, undesirable to say the least. As laser light is generally highly polarized, the digital bits that they emit contain light that is also highly polarized. Couple this with the birefringence present in the fiber and the result is that different components (polarizations) of the digital bits travel at different velocities (27). In other words some of the light in the bit travels faster and some of the light travels slower. This causes the digital bit to spread in time; this is termed dispersion. Moreover, the residual birefringence is not constant along the length of the fiber but changes with distance in a random way, not only in amount, but also in its local principal axes. For a given fiber, PMD is supposed to be fixed. However, this is not the case in real systems because environment fluctuations cause PMD to vary randomly in time. Therefore, it is important to understand the statistical properties of pulse propagation induced by PMD.

4.2 Impacts of Polarization Mode Dispersion on the performance of Optical communication system

In this part, two systems at different bit-rate are studied, to show how the PMD can degrade a system performance; the first system is built using an older fiber with an high PMD coefficient, while the second one is built with new fiber with less PMD coefficient than the previous one.

Chromatic dispersion and Non linear effects have been disabled, so that all the variation of the results is due to PMD .

The bit rate is varied from 10 Gbps to 40 Gbps and the simulations are made with or without PMD coefficient, to show how the polarization mode dispersion affect a communication system.

It is shown that the impact of PMD increases with the bit rate of system. It is also observed that the impact of PMD becomes intolerable at the bit rate of more than 40 Gbps. Also the PMD produces very minute impact on the system performance for same bit rate with the variation in the fiber length.

4.2.1 Simulation Setup

The system architecture shown in Fig. 4.1, is build to study the impacts of Polarization Mode Dispersion over different bit rates. In the setup two simple optical transmission systems are compared on the basis of fiber PMD coefficient and bit-rates, to find the maximum distance that can be reached with a bit error rate of 10^{-10} and 10^{-4}. It's taken in account also the a value of 10^{-4} for the BER, because with the FEC (Forward Error Correction) it could possible to improve the BER from a value of 10^{-4} to 10^{-10}.

In the transmission side the signal generator generates a pseudo random data sequences in order to emulate a real data transmission; subsequently the data sequence is coded by a NRZ Coder that generates for each input bit, an electrical Non Return to Zero coded signal. At this point the coded signal is filtered by a

Gaussian filter that transforms, rectangular electrical input pulses into smoother output pulses with a user-defined rise-time. Its effect is to band-limit the modulated optical signal, which is required to avoid numerical artefacts when resampling to higher sample rates.
After these steps, a Mach Zehnder modulator modulates the optical carrier signal from the laser source with the electrical signal from the signal generator, in order to obtain an optic source that comes through the fiber.

The two fibers type, that are used in this simulation, have a PMD coefficient of $0.5\ ^{ps}/_{\sqrt{Km}}$ and $0.1\ ^{ps}/_{\sqrt{Km}}$ respectively; and the PMD emulation is made under the worst case condition, that is with the power-splitting of the two polarization set equal to 0.5, that provides the worst waveform distortions. Only the attenuation (0,2 dB/Km) is taken in account, while chromatic dispersion and non linear effects are sets to be negligible.

At the receiver side, the fiber is connected to a PIN photo detector that converts the optical signal into an electrical one. The electrical output of the photo detector is filtered by a Bessel Low-pass filter; the aim of this module is to remove all spectral components located beyond a corner frequency, passing only a defined band of frequencies.

The filter's output is connected to a Ber estimator, that estimates the bit error ratio (BER), and the results are plotted by the graphical analyzer.

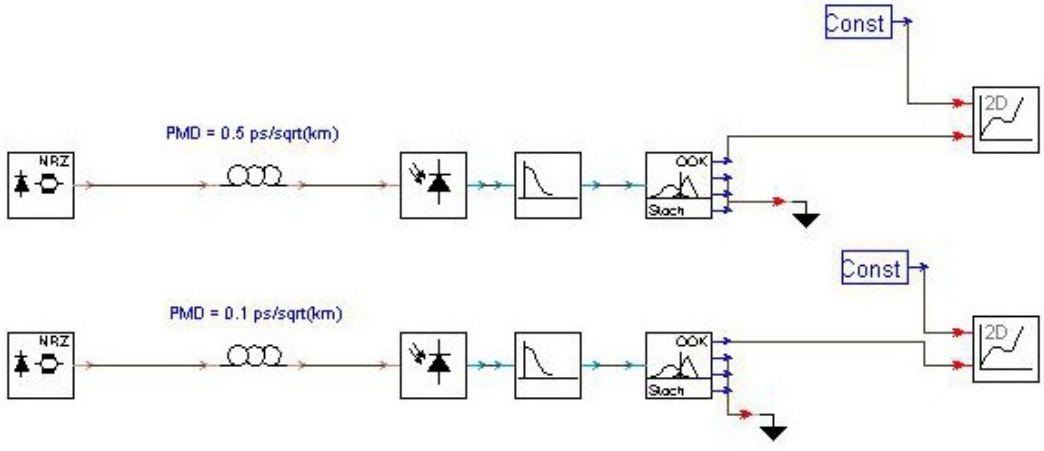

Figure 4.1 Simulation setup

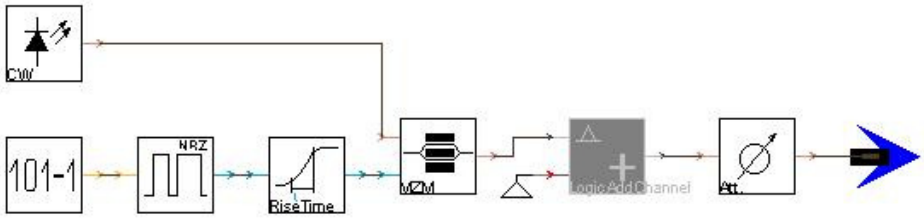

Figure 4.2 Transmitter's scheme

Component	Parameter	Value
Transmissor	Bit-rate	10 - 40 Gbps
	Laser Frequency	193.1 THz
	Laser Average Power	1 – 2 mW
	Laser ellipticity	0
	Rise time	0.25/Bit-rate
Fiber	Attenuation	0.2 dB/Km
	Chromatic Disp.	0
	Disp. Slope	0
	Non linear index	0
	Core Area	$80e^{-12}\ m^2$
	PMD coefficient	$0.5 – 0.1\ ^{ps}/_{\sqrt{Km}}$
	Power split ratio	0.5
Receiver	Photodiode type	PIN
	Responsivity	1
Electrical filter	Filter type	Low pass
	Transf. function	Bessel
	Bandwith	0.7*Bit-rate
	Order	4

Table 4.1 Scheme parameters

4.2.2 Simulations results and comments

In this section are been reported the impacts of Polarization Mode Dispersion over the length (at different bit-rate) in an optical network transmission.

4.2.2.1 Only PMD

As mentioned in Section 2.7, according to equation 2.17, $B^2L = \frac{0.020}{(PMD)^2}$ the maximum reachable length of a fiber with only PMD and without other impairments, is inversely proportional to the bit-rate and to the PMD coefficient.

In this first simulation these theoretical limits are investigated to see how the maximum achievable distances are reduced significantly with increasing bit-rate of the system or increase the PMD coefficient of the fiber. These distances are a theoretical one, that is impossible to reach in real system.

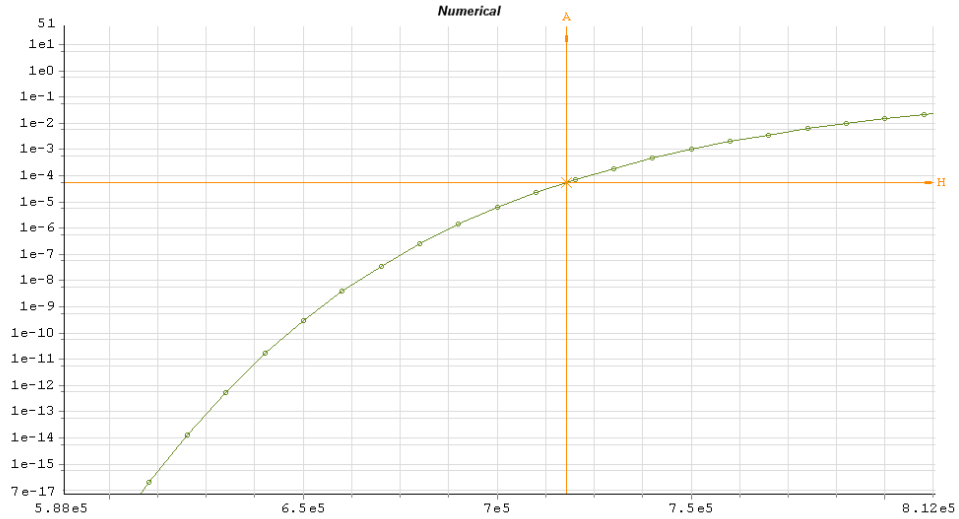

Figure 4.3 PMD = 0.5 ps/sqrt(Km) Bit-rate = 10 Gbps

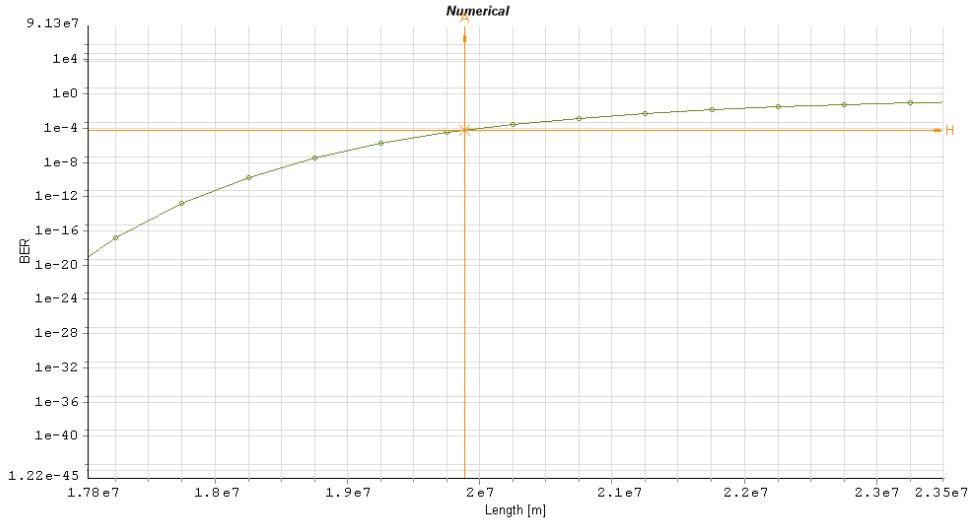

Figure 4.4 PMD = 0.1 ps/sqrt(Km) Bit-rate = 10 Gbps

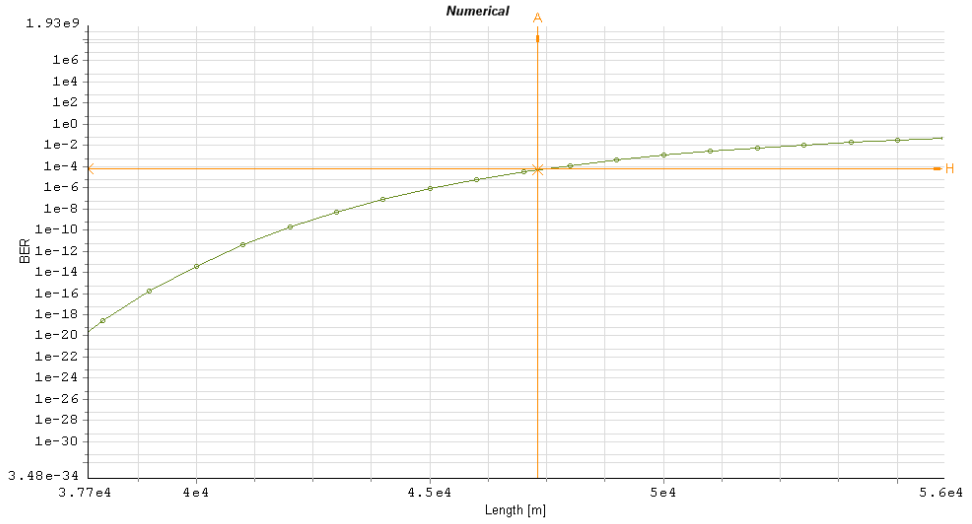

Figure 4.5 PMD = 0.5 ps/sqrt(Km) Bit-rate = 40 Gbps

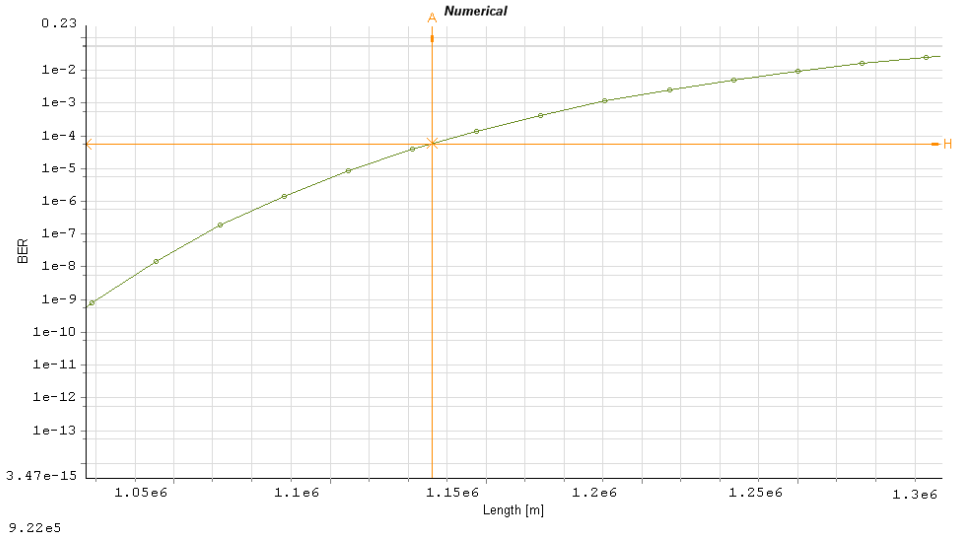

Figure 4.6 PMD = 0.1 ps/sqrt(Km) Bit-rate = 40 Gbps

Bit- rate [Gbps]	Maximum Length [Km] PMD_c=0.5	Maximum Length [Km] PMD_c=0.1
10	717	19800
40	47	1144

Table 4.2 Theoretical PMD limits

As it can be seen from the results of this first simulation, the theoretical limits imposed by PMD vary widely depending on the bit-rate. This initial result can be explain how PMD can affect a transmission, reducing the maximum achievable distance, at which a proper reception of the signal could be done. At 10 Gbps the maximum distance varies of a value of 19000 Km changing the PMD coefficient from $0.5\ ^{ps}/_{\sqrt{Km}}$ to $0.1\ ^{ps}/_{\sqrt{Km}}$; while at 40 Gbps, respect the previous case with a coefficient of $0.5\ ^{ps}/_{\sqrt{Km}}$ the maximum achievable distance cannot exceed the distance of 47 Km, with a difference of almost 670 Km; and with a coefficient of $0.1\ ^{ps}/_{\sqrt{Km}}$ the difference with the transmission at 10 Gbps is about 18600 Km.

These data are not a real one, because in reality we have to face with some stronger limitation like the fiber's attenuation, chromatic dispersion and non linear effects. On the base of this assertion, a more real simulation is performed, to see the real effects, and the real limitation imposed by polarization mode dispersion.

4.2.2.2 Effects of Attenuation and PMD

After a first completely theoretical simulation, it will be to investigate the performance of the transmission with only fiber's attenuation before, and then will also be added the PMD.
Simulations were made with a transmitting power of 0dBm and 3dBm in order to assess whether the benefits vary linearly or less, depending on the transmitted power.

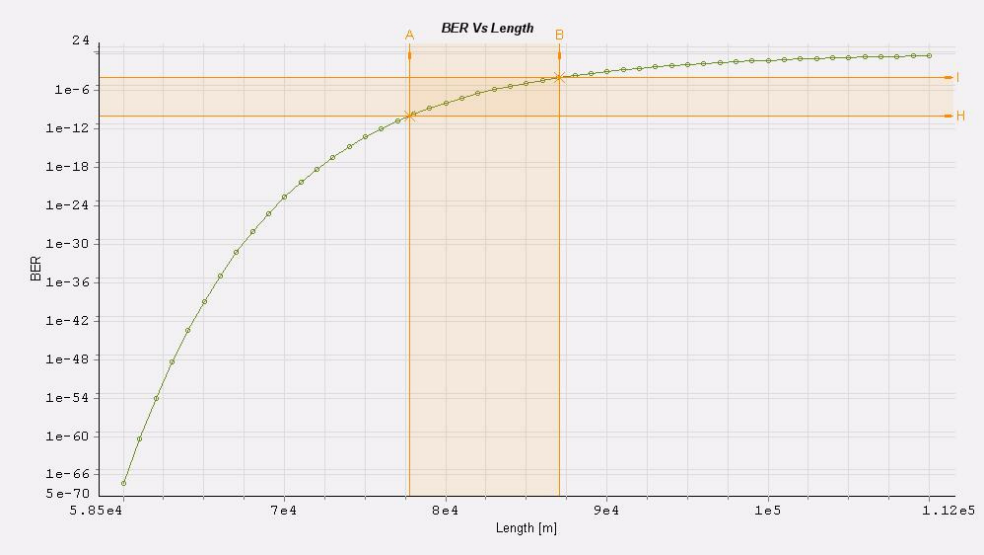

Figure 4.7 Bitrate=10 Gbps, No PMD

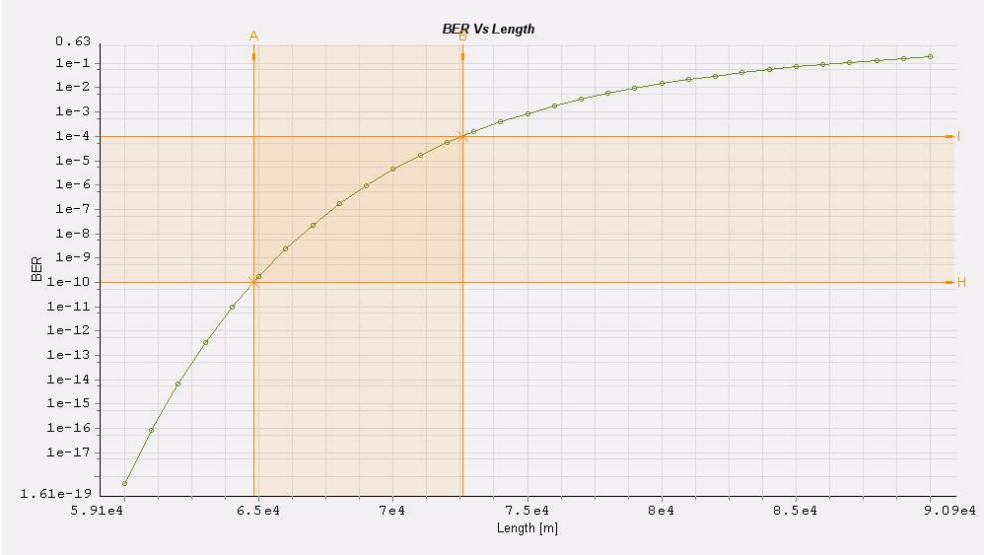

Figure 4.8 Bitrate=10 Gbps, PMD=0.5 ps/sqrt(km)

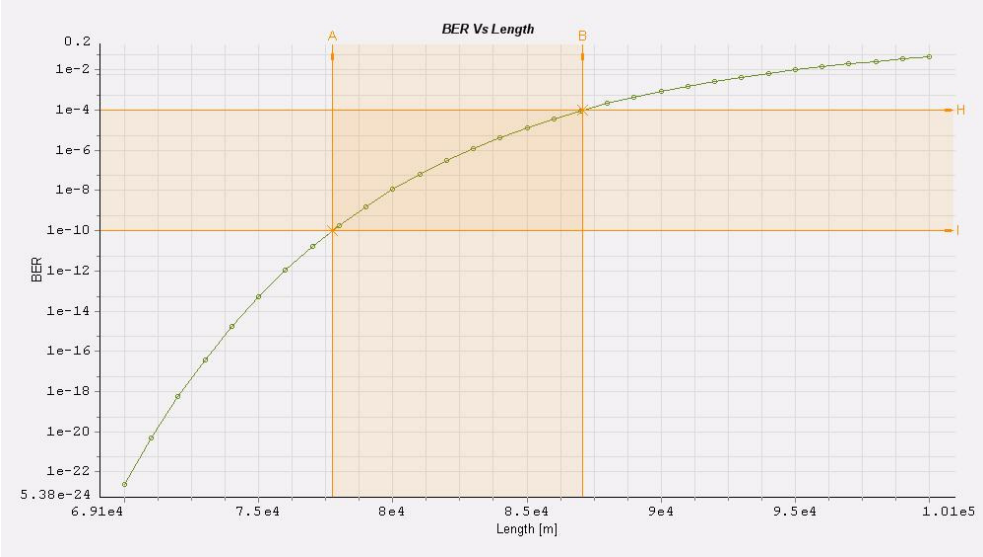

Figure 4.9 Bitrate=10 Gbps, PMD=0.1 ps/sqrt(km)

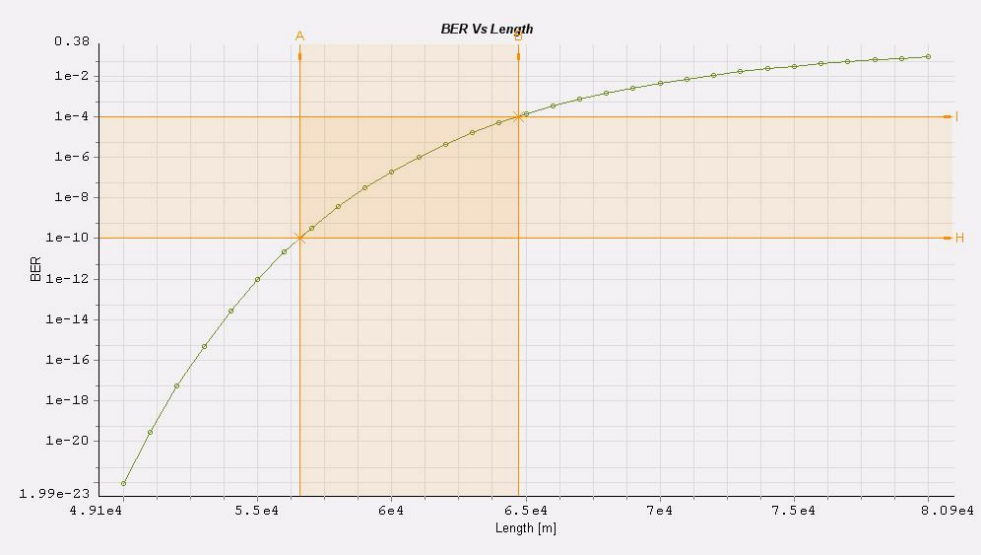

Figure 4.10 Bitrate=40 Gbps, no PMD

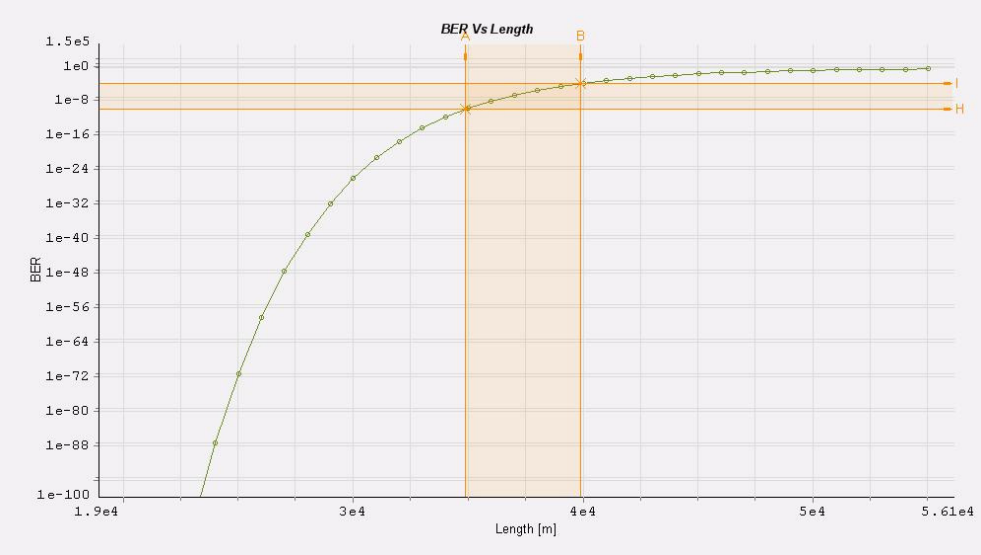

Figure 4.11 Bitrate=40 Gbps, PMD=0.5 ps/sqrt(km)

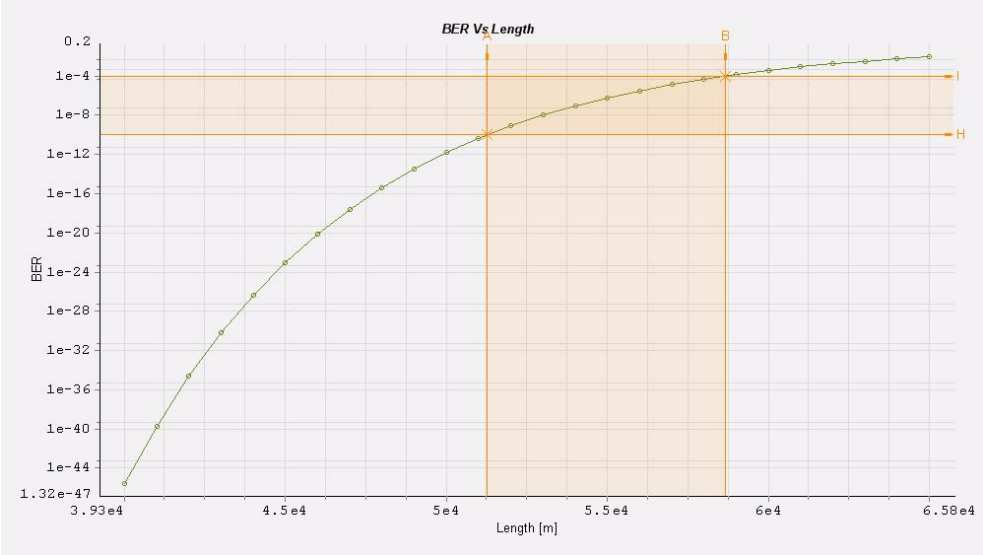

Figure 4.12 Bitrate=40 Gbps, PMD=0.1 ps/sqrt(km)

In the table below are summarized the simulation's results.

Bit Rate [Gbps]	Transmission Power [dBm]	PMD Coefficient $[^{ps}/_{\sqrt{Km}}]$	Ber Vs Length		Ber Bs Received Power	
			L [Km] @Ber=10^{-3}	L [Km] @Ber=10^{-10}	L [Km] @Ber=10^{-3}	L [Km] @Ber=10^{-10}
10	0	0	87	77	-17,4	-15,5
		0.5	72	65	-14,5	-13
		0.1	87	77	-17,4	-15,4
	3	0	99	75	-16,8	-15
		0.5	89	68	-14,8	-13,6
		0.1	99	74	-16,8	-14,8
40	0	0	64	56	-12,8	-11,3
		0.5	40	35	-7.9	-7
		0.1	59	51	-12.4	-10,3
	3	0	83	59	-13,6	-11,8
		0.5	57	37	-8,4	-7,4
		0.1	75	53	-12	-10,5

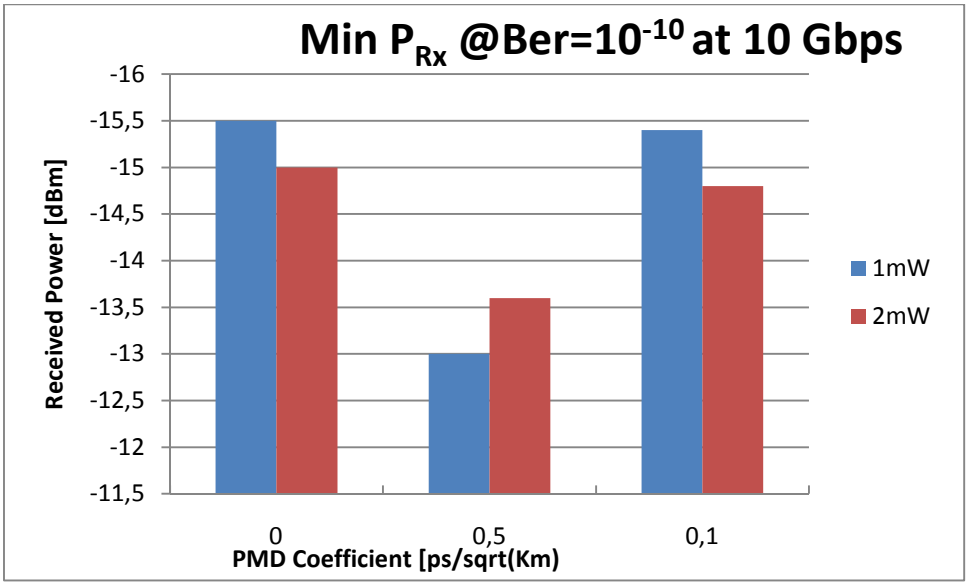

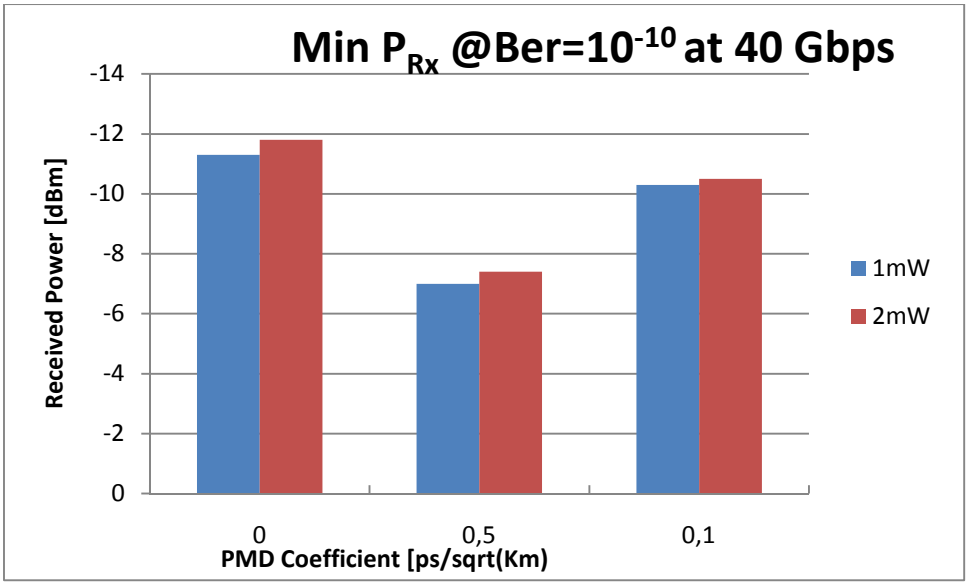

From the obtained results, the first thing that can be noted is that in function of the optical power transmitted , the distance varies linearly in both cases, with or without PMD. Henceforth, for simplicity, all simulations will be performed by transmitting a power of 1 mW.

The second thing that can be noted is how the PMD affects a transmission system, especially at high bit-rate.

In the system with bit-rate of 10 Gbps, it can be seen how the PMD affects the transmission distance only with high coefficients (0.5 ps / √ km) where it begins to reduce the maximum achievable distance compared to the case without PMD or with low coefficient (0.1ps / √ km).

Instead in the previous case, in the system with bit rate of 40 Gbps, the effect of PMD starts to become much more important. In fact, this impairments can paralyze an optical communication system with high PMD coefficient (0.5 ps / √ km), blocking transmissions over distances of greater than 40 km, while beginning to reduce even slightly the maximum distance reached by fiber with a low PMD coefficient (0.1ps / √ km) in a single span.

Except the transmission at 40 Gbps with a fiber's PMD value of 0.5ps / √ km, in all other cases tested, the major limitation on the maximum achievable distance is given from the fiber's attenuation, because the maximum attainable value distance have the same level.

For this reason, in the next part of this chapter, it will be analyzed the maximum lengths obtained by compensating the attenuation of the various sections of fiber, so as to study the real performance of the effect of PMD.

4.2.3 Multispan

4.2.3.1 Simulation setup

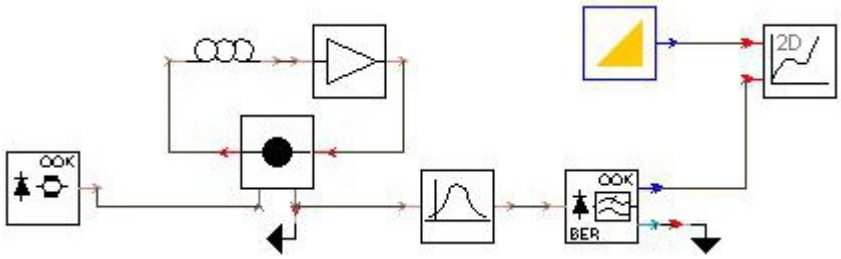

Figure 4.13 Multi span setup

In the previous figure above is represented the simulation's scheme; instead of the simple optic fiber there is a loop, that simulates a system with fiber and an amplifier in series. The amplifier's gain is set to recovery the attenuation gives from the previous fiber's section. At the end of the entire series of fiber-amplifier there is an optical Gaussian band-pass filter, that remove the out of band amplified spontaneous emission (ASE) noise, coming from the amplifier; and at the end, like in the previous simulation there is a ber estimator.

4.2.3.2 Multispan results at 10Gbps

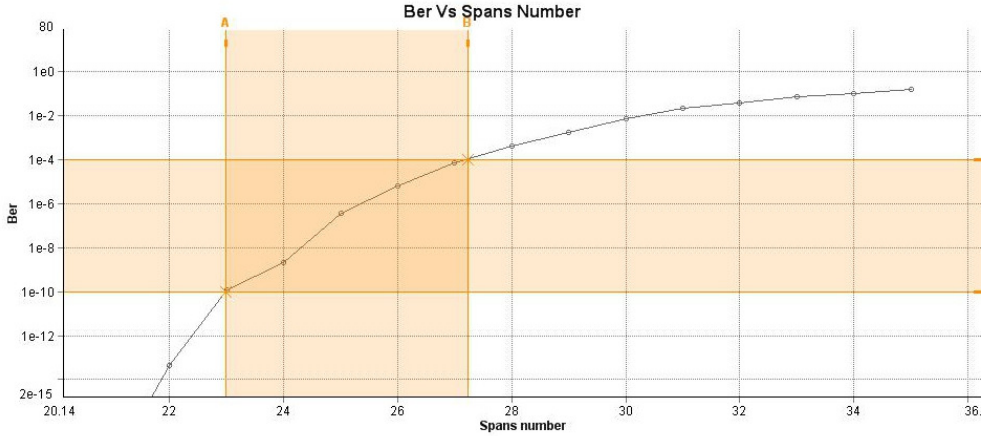

Figure 4.14 PMD= 0 ps/sqrt(Km) Bit-rate = 10 Gbps

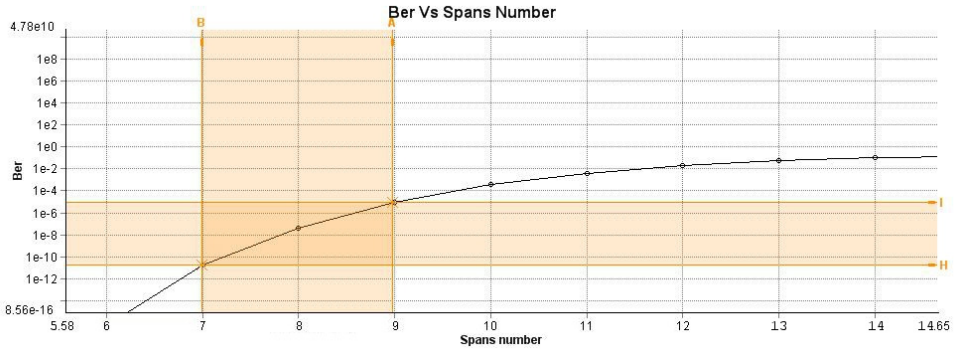

Figure 4.15 PMD= 0.5 ps/sqrt(Km) Bit-rate = 10 Gbps

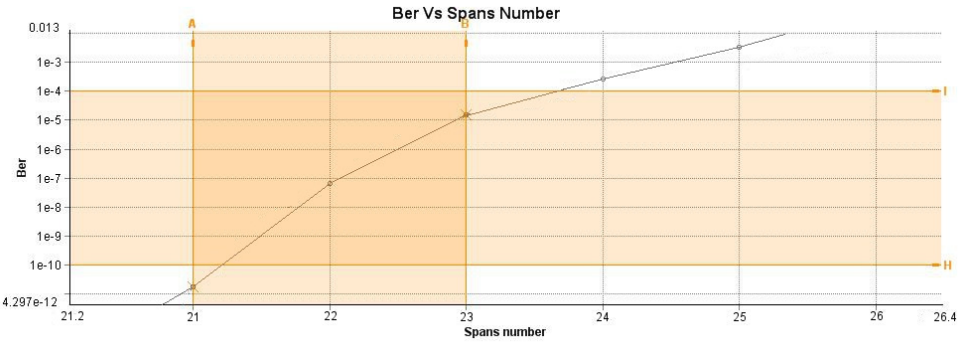

Figure 4.16 PMD= 0.1 ps/sqrt(Km) Bit-rate = 10 Gbps

4.2.3.3 Multispan results at 40Gbps

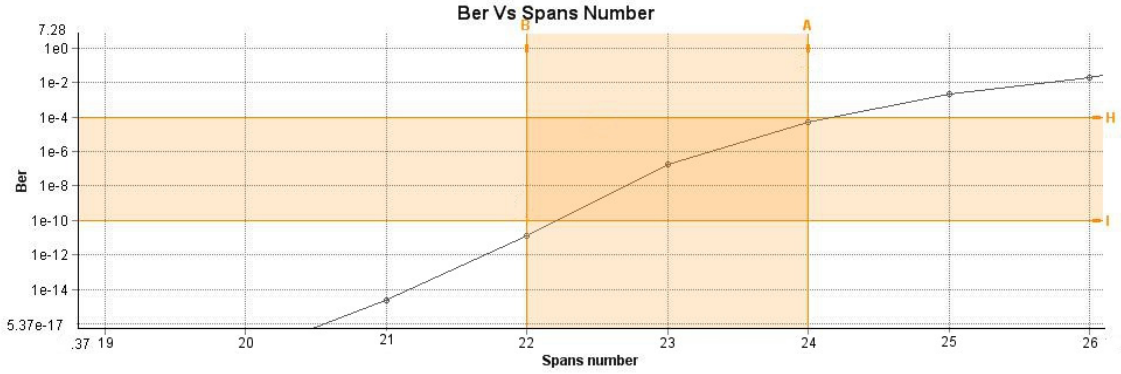

Figure 4.17 PMD= 0 ps/sqrt(Km) Bit-rate = 40 Gbps

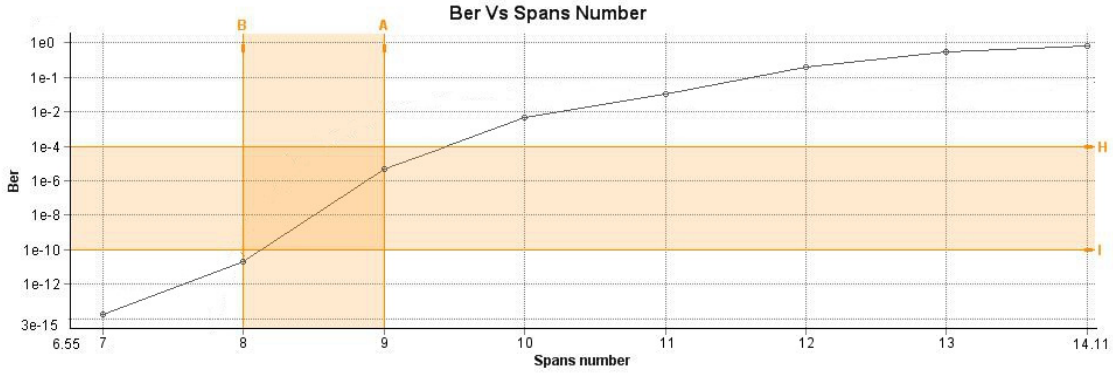

Figure 4.18 PMD= 0.1 ps/sqrt(Km) Bit-rate = 40 Gbps

Bit Rate [Gbps]	PMD Coefficient $[^{ps}/_{\sqrt{Km}}]$	Length [Km]		Span length [Km]	N° of spans	
		@Ber=10^{-4}	@Ber=10^{-10}		@Ber=10^{-3}	@Ber=10^{-10}
10	0	1690	1495	65	26	23
	0.5	550	450	50	9	7
	0.1	1495	1365	65	23	21
40	0	1080	990	45	24	22
	0.1	495	450	45	11	10

Table 4.3 Multi-span results

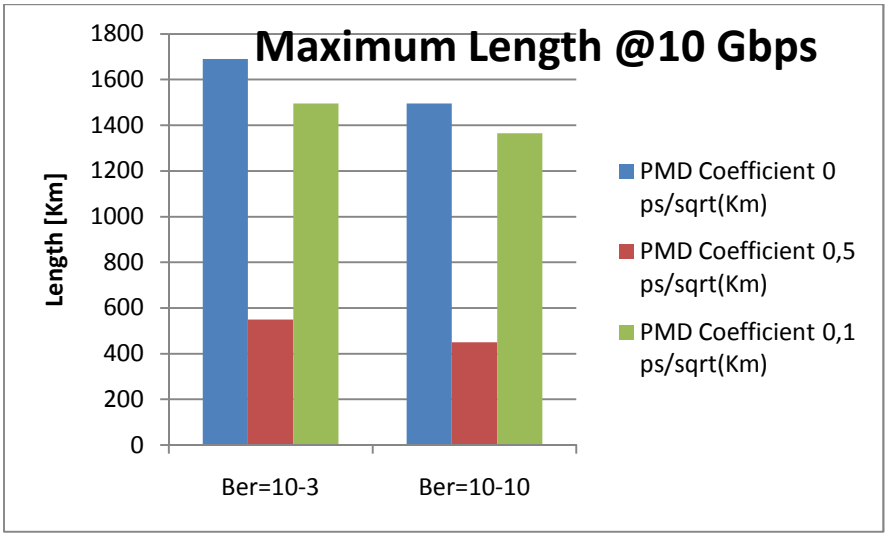

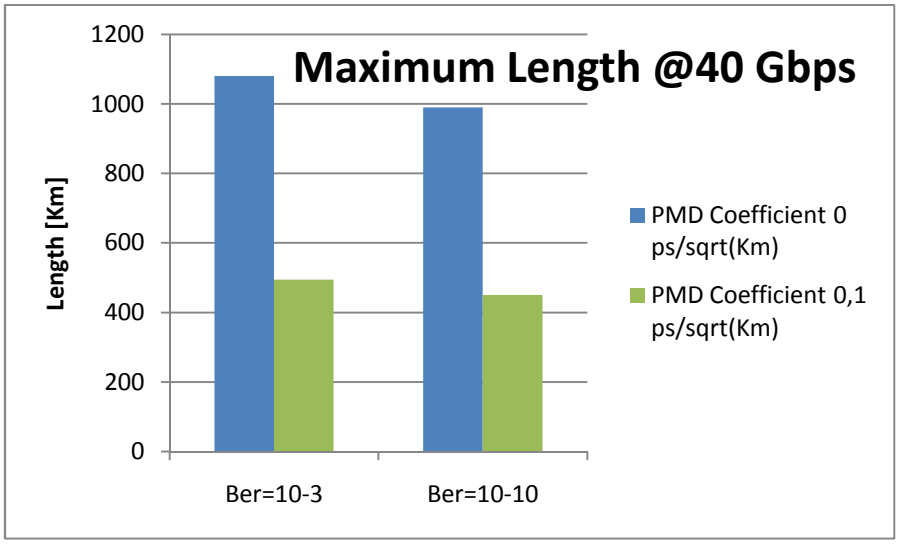

From these data it can be demonstrated how, in a long-haul system, the PMD can affected the transmission capacity.

In the first case, with a transmission's bit-rate of 10 Gbps, in an old fiber with a coefficient of 0.5 $^{ps}/_{\sqrt{Km}}$ the performance are limited, and the maximum reachable distance is about an half respect of the other fibers, while in the system with a lower PMD coefficient the impact of PMD is less evident, with a decrease of maximum reach distance of a few kilometers.

In the second case, when the transmission is made with a bit-rate of 40 Gbps, an high PMD coefficient in the fiber completely block the transmission, while limit in a quite strong manner the link with a PMD coefficient of 0.$^{ps}/_{\sqrt{Km}}$1.

4.3 **Forward Error Control**

As said at the beginning of this chapter, in accordance with the theory of paragraph 3.3 it's possible to extend the maximum achievable distance with the use of a Forward Error Control after the receiver. This electronic element can improve the Bit Error Rate, passing from a value of ~10^{-4} to 10^{-10}; this means that the maximum achievable distance can be increased. In the following simulation is shown the Fec's effects applied to the transmission at 10 Gbps with transmission power of 0 dBm and a PMD coefficient of 0.1$^{ps}/_{\sqrt{Km}}$.

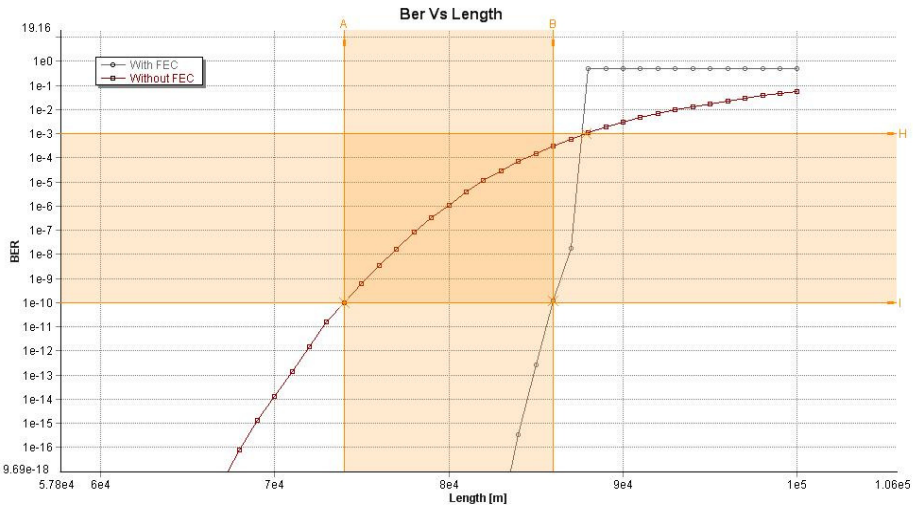

4.19 Transmission comparison with and without FEC

From the previous graph (Fig. 4.19), it can be seen how the FEC works until a value of 10^{-3} improving the Ber, passing from ~10^{-4} to 10^{-10}. Above a value of 10^{-3} the FEC cannot works and gives a constant value of 0.5.
With this technique is possible to have a little improve of the system performance, and in some cases its avoid the use of a PMD compensator, but in most cases, the use of this technique is not enough.

4.4 **Conclusion**

Form the above results it is observed that Polarization Mode Dispersion puts more impact over the system as the bit rate increases. The older fibers having the PMD coefficient of 0.5 $^{ps}/_{\sqrt{Km}}$. shows the performance degradation with increase in bit rate. But as the new fibers have reduced PMD coefficient up to 0.1 $^{ps}/_{\sqrt{Km}}$. also puts impact to degrade the signal quality of the communication system. At 10 Gbps PMD is no more negligible however at higher bit-rates of 40 Gbps and above, it represents the major limitation in optical transmission systems. So if we have to move further to the higher bit rates, the PMD mitigation is necessary.

CHAPTER 5
PMD COMPENSATION

5.1 Introduction

As noted in the previous chapter, polarization mode dispersion is one of the major limiting factors for high-speed optical communication systems; it paralyses the transmission at 40 Gbps and also highly degrades the transmission at 10 Gbps over long fiber spans.
Due to this factor, in the new high-speed optical systems, a PMD compensation is needed.
In the first section is simulated a first-order PMD compensator, and a monitor signal that can be used in an adaptative compensator, in system with different bit-rate, in order to show how this compensator works.

In the second one, the compensation is applied to the previous multi-span system, to study how the performance of a system get increasing with a PMD compensation; while in the last one the system tolerance to PMD with or without compensation is investigated.

5.2 Compensator

A technique design for compensation of first-order polarization-mode dispersion (PMD) is proposed. Simulations show that the effects of the high-PMD long-haul fiber are dynamically mitigated or minimized and that the data are recovered from the distorted signals. The resulting apparatus will enhance the transmission quality, and extend the maximum reachable distance. This system provide a dynamically reconfigurable functional control to mitigate the influence of PMD fiber on high-bit-rate optical data.

5.2.1 PMD Monitor

As a part of a feedback system, the PMD monitoring circuit is used to measure the PMD level and provide feedback to the control circuit of the compensator. For PMD monitoring, a widely used technique measures the power spectral densities (PSDs) at certain frequencies and uses those measurements as an indicator of the PMD level.

The theory at the basis of this technique is that the PSD is proportional to the following expression:

$$P_{monitor} \propto 1 - \gamma(1-\gamma)(2\pi f_c \Delta\tau)^2$$

where, γ is the ratio of power-splitting between the two input PSPs, is the center frequency of the band-pass filter for extracting the monitor signal and is the net DGD. The waveform distortion caused by first order PMD of the transmission line can be quantified by a set of the three parameters: group delay difference , power ratio between the two principal states of polarization, and the center frequency of the band-pass filter for extracting the monitor signal.

The transmission is made with a power-splitting , that is the worst case and a medium case, in which the total transmitted power is equally divided into the two polarization gives the worst possible waveform distortion ( ), and another case in which the 75% of the power goes into a polarization mode (.

The frequency component at the half-bit-rate frequency is extracted from the base-band signal spectrum by a narrow-bandpass filter; so the relation between the intensity of this signal (PSD) and the PMD coefficients is explored, to optimize the PSD as a function of PMD.

For this purpose the following schematic was designed, and each block represents the labeled device or subsystems whose characteristics and parameter can be modified to simulate the model, in a manner quite close to that of the real device and the respective response functions.

5.2.1.1 Simulation setup

For this simulation, to investigate the effects of the PMD over the PSD, the PMD coefficient in the fiber were changed in order to achieve different value of DGD, at the receiver from 0ps to 25ps; and the power ratio γ was set at 0.5 and 0.25 in order to see how the PSD varies, varying the power ratio between the two polarization axes.

The monitor signal is taken at an half of the bit-rate frequency (for transmission at 10Gbps the signal is taken at 5GHz, while at 40 Gbps is taken at 20 GHz). The PMD fiber model includes DGD and the higher orders of the PMD as well. Since the signal is attenuated after propagating through the long-haul fiber, an amplifier is incorporated to boost the optical signal before the signal goes to the monitoring circuit.

At the transmission side an NRZ signal is modulated trough a Mach-Zehnder modulator, at a rate of 10 or 40Gbps.

At the end of this transmission line the photo-detector is a PIN type, and the band-pass filter is set to have the central frequency at an half of the bit-rate. After the filter a power meter measure the power level of the spectrum, and the results are plotted in a graph.

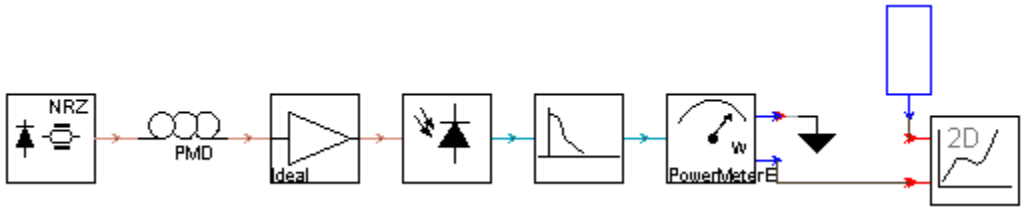

Figure 5.1 Monitor signal setup

5.2.1.2 Result and discussion

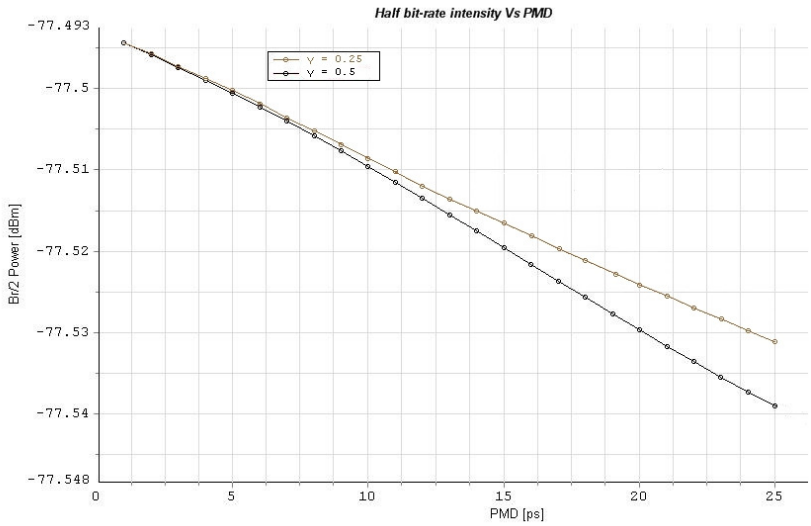

Figure 5.2 5-GHz intensity as a function of $\Delta\tau$

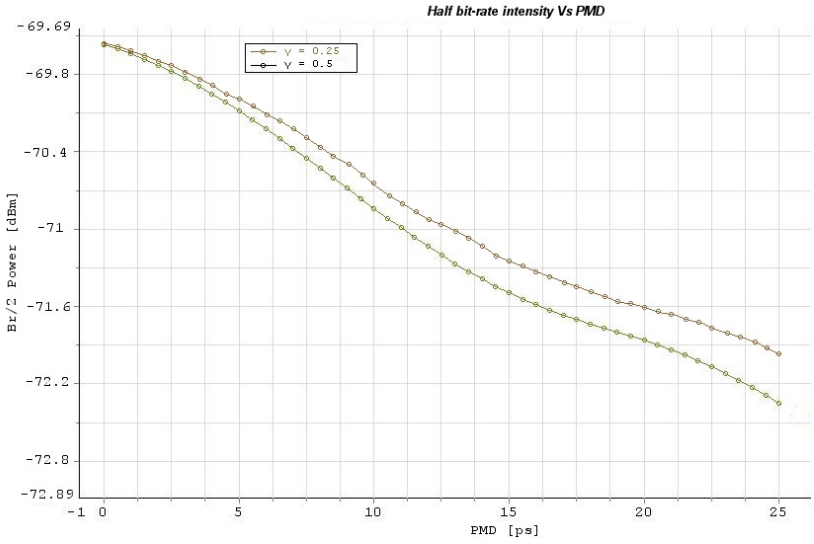

Figure 5.3 20-GHz intensity as a function of $\Delta\tau$

As shown in the above figures, the intensity of the monitor signal is decreasing for increasing PMD coefficients; and It is experimentally confirmed that a bit-rate/2 signal intensity is proportional to $P(f_c)$, where f_c is the frequency extracted from the baseband signal.

This inverse proportionality between the half-bit-rate frequency intensity and the PMD coefficient is quite monotonic, the intensity is highest at $\Delta\tau = 0ps$ and decrease up to $25ps$.

It's expected that, where $\boldsymbol{\Delta\tau}$ is less than $25ps$, the distorted waveform caused by PMD will be recovered by maximizing the half bit-rate intensity using a PMD compensator.

5.2.2 Compensator

In this system the compensation is made through a polarization rotator, and a fixed delay line. The polarization rotator is used to rotate the SOP of the lightwave, to controls which component of the light is to be delayed, as discussed above.

Fig. 5.5 shows the schematic of this optical system. The schematic uses the PMD emulator shown in Fig. 5.4 that emulates the PMD effects in fiber. The delay line has a constant variable delay added to one of the components. The polarization controller rotates the SOP of the incoming light by different angles, and the effect of this rotation on the eye diagram of the received signal is observed on the oscilloscope. The simulation was run for different DGDs in the emulator, and for each DGD value, the rotation-angle of polarization rotator was swept from –90° to 90° to cover the complete range of SOP.

5.2.2.1 Simulation setup

To investigate the performance of a PMD compensator, two different series of simulation are made at different bit-rate (10 Gbps and 40 Gbps) and with different value of DGD. Only the effects of PMD is taken in account, all the other dispersion are set to be negligible..

In the fig. 5.4 it can be seen the PMD emulator. The transmitter side is like in the previous simulation, a NRZ modulator is used with a laser that works in the third windows @1,553 nm with different bit-rate @10Gbps and 40 Gbps.

The main target of this modulation format is to improve PMD compensation as said in chapter **2** when this problem was analyzed.

In order to be able to works many times over the same transmitted data, the generated signals from the transmitter are not immediately processed by the compensator , but they are first saved to a file (Fig. 5.4).

There were made several simulation varying the DGD value reached at the end of the fibers, in order to simulate at 10 an 40 Gbps a DGD value of 5, 10, 15, 20 and 25 *ps.*

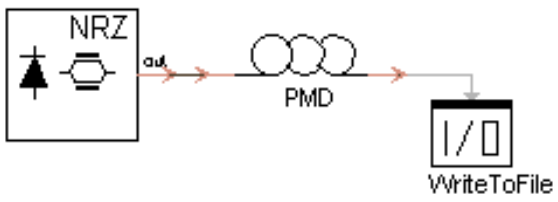

Figure 5.4 Pmd Emulator

After this first step, in the compensator setup (Fig. 5.5) the collected data are read from the file. After that, there is a signal bifurcations of the incoming signals, on one side the signals goes to the compensator, and after a compensation is received from a photodiode, filtered from a low-pass filter and re-clocked after

that it could be analyzed; when on the other side is the same, but the signal is not compensated. This is made due to compare the compensated signal with the uncompensated one.

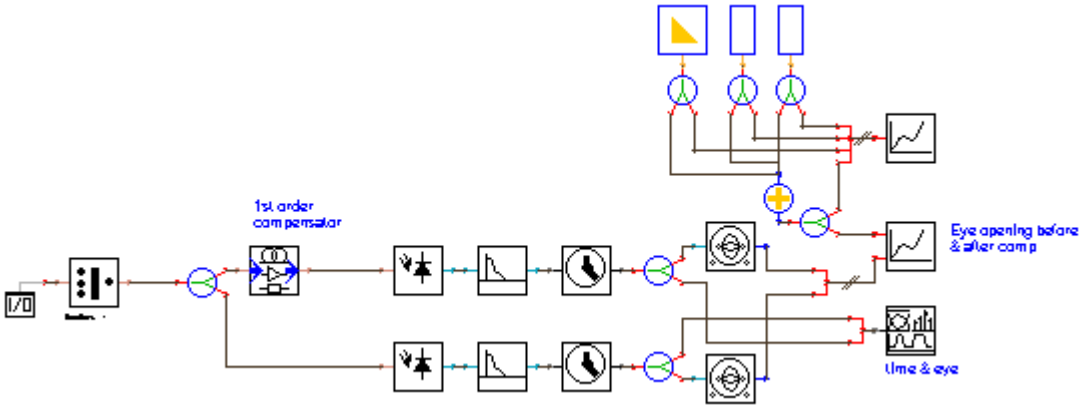

Figure 5.5 Compensator setup

5.2.3 Simulation's results and comments

In this chapter the performance of a PMD compensator have been reported. For reference and comparison Fig. 5.6 shown the eye diagram of the signal before the segment of optical fiber. The attenuation parameters in the fiber were set to be negligible.

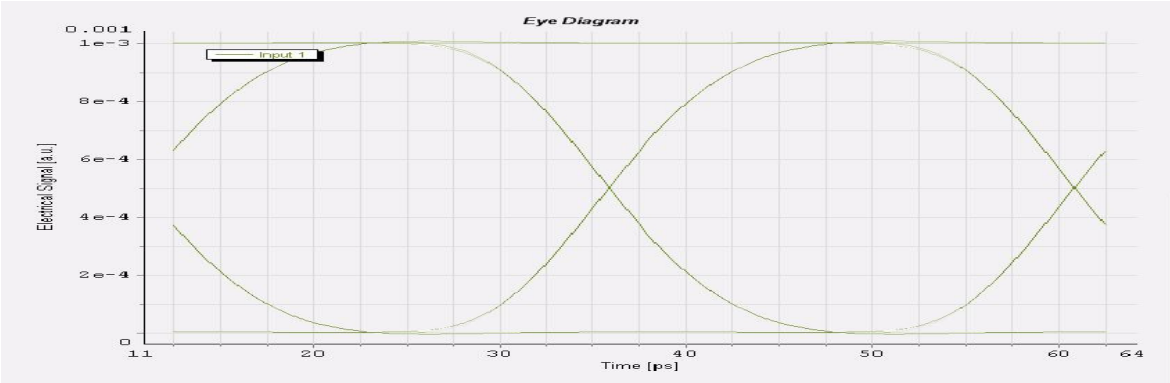

Figure 5.6 Eye diagram before the fibre

5.2.3.1 Simulations at 10Gbps

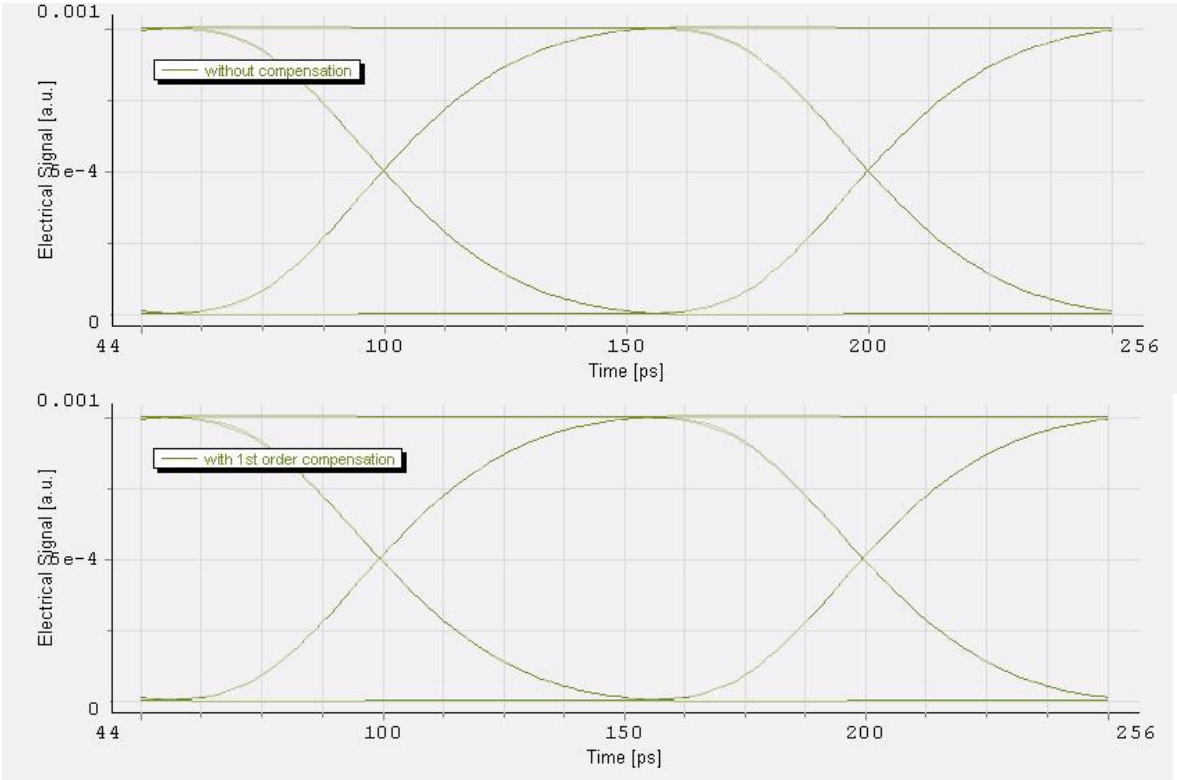

Figure 5.7 Eye Opening With or Without First Order Compensation @10Gbps with a Mean DGD value of ~5 ps

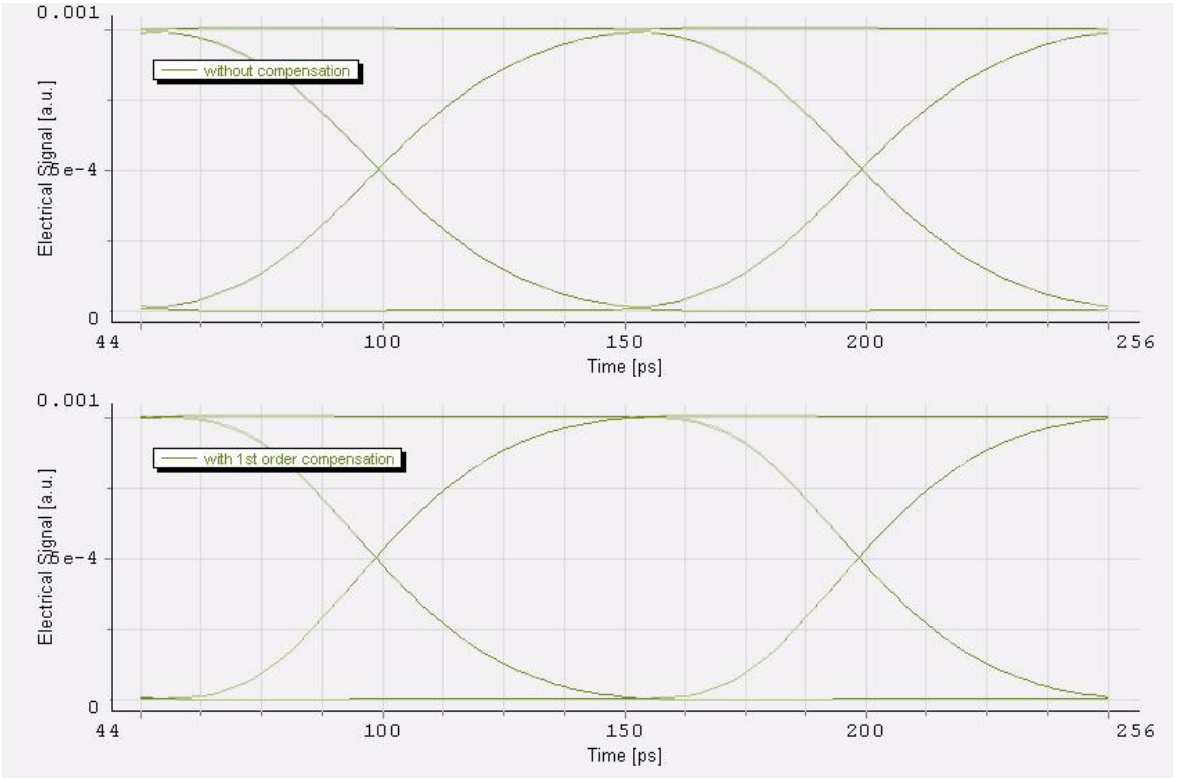

Figure 5.8 Eye Opening With or Without First Order Compensation @10Gbps with a Mean DGD value of ~10 ps

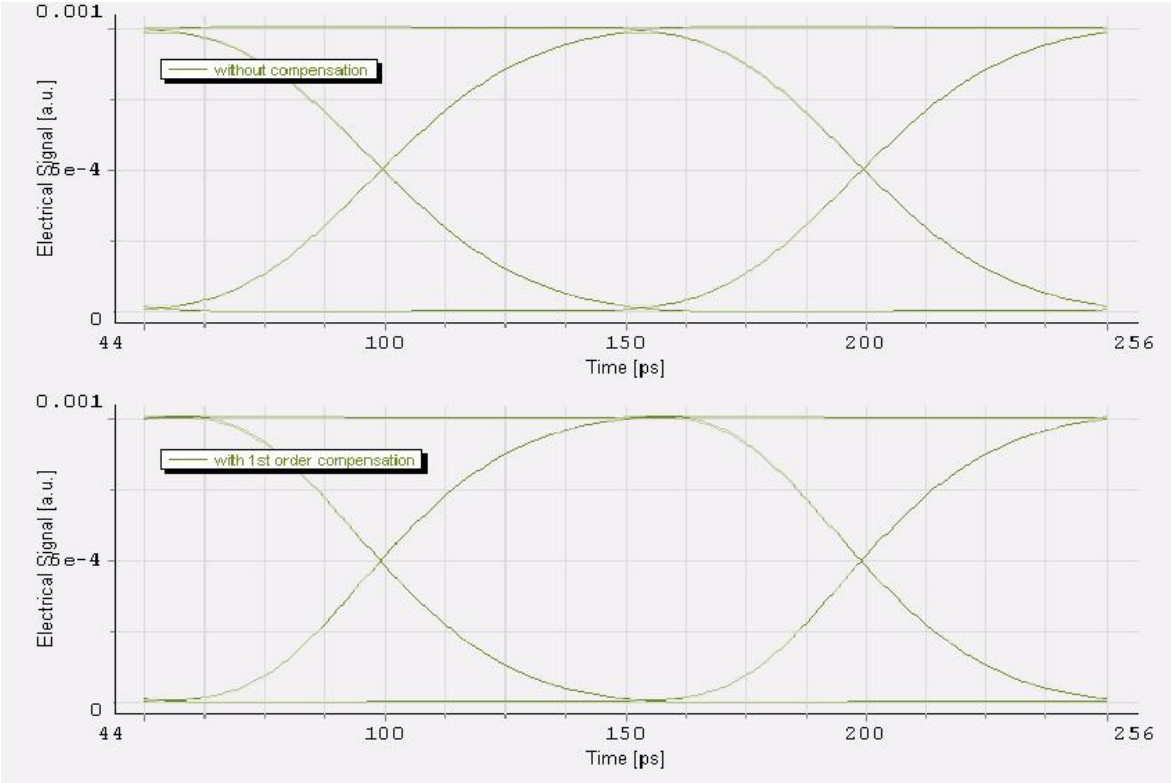

Figure 5.9 Eye Opening With or Without First Order Compensation @10Gbps with a Mean DGD value of ~15 ps

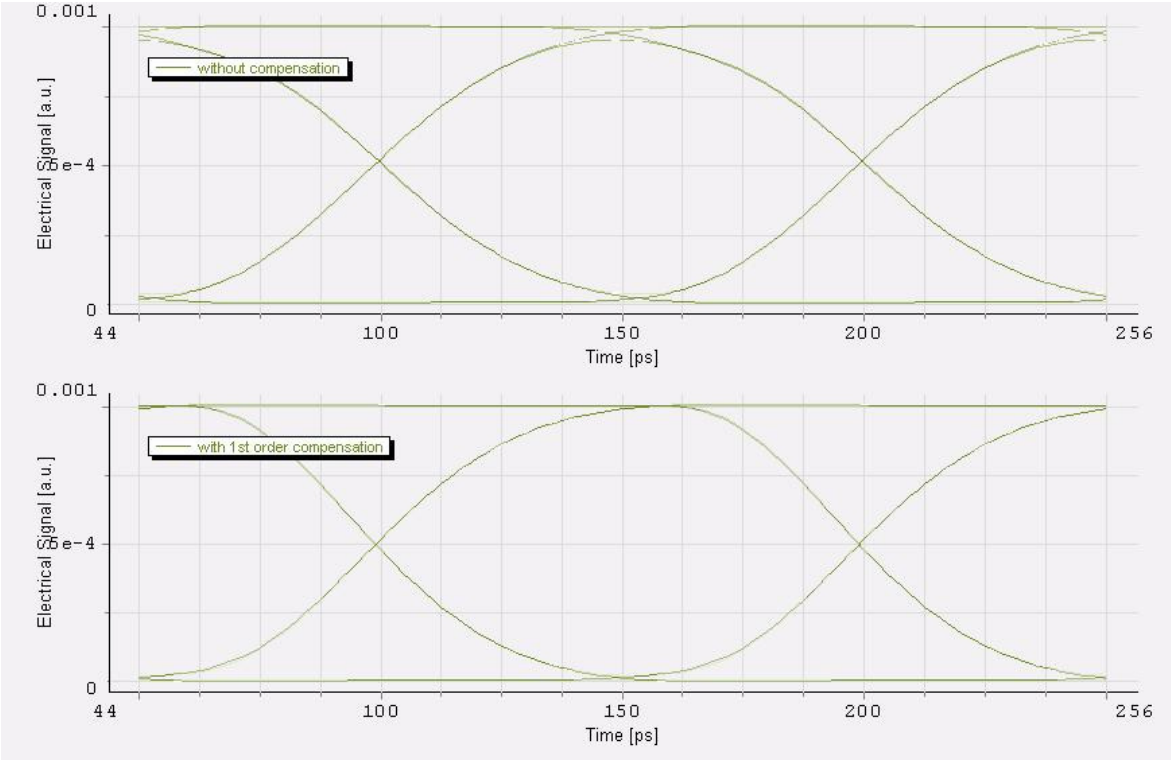

Figure 5.10 Eye Opening With or Without First Order Compensation @10Gbps with a Mean DGD value of ~20 ps

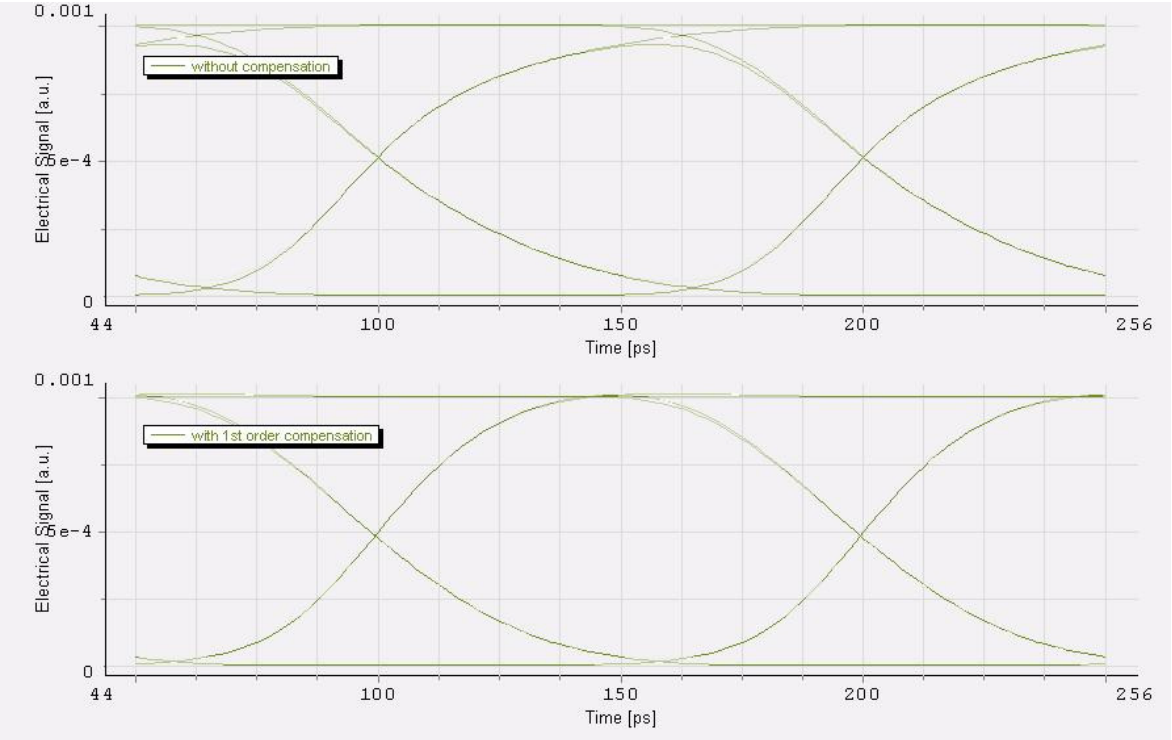

Figure 5.11 Eye Opening With or Without First Order Compensation @10Gbps with a Mean DGD value of ~25 ps

5.2.3.2 Simulations at 40 Gbps

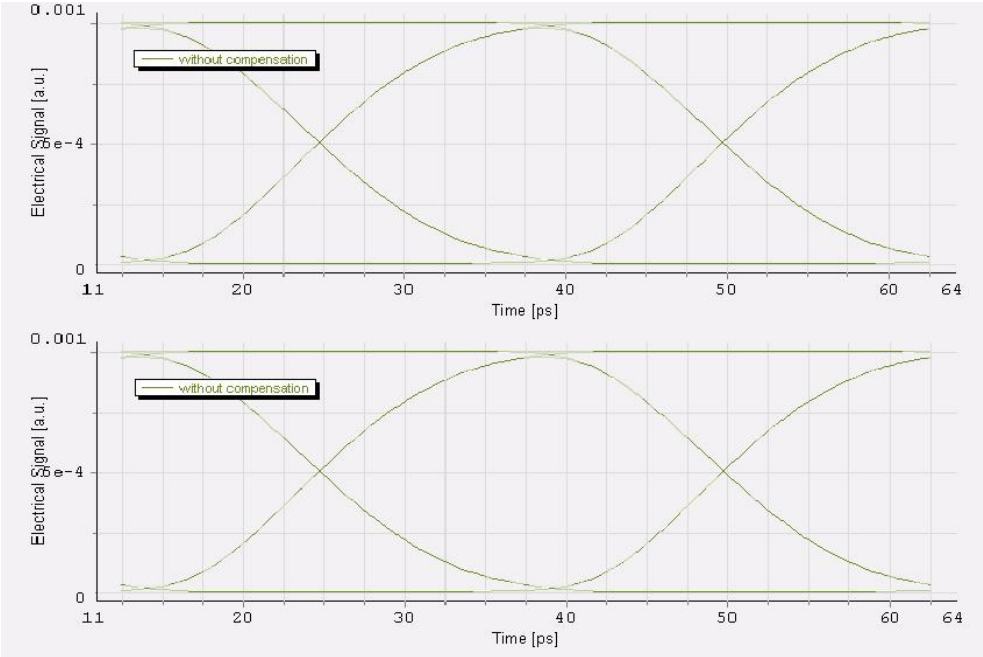

Figure 5.12 Eye Opening With or Without First Order Compensation @40Gbps with a Mean DGD value of ~5 ps

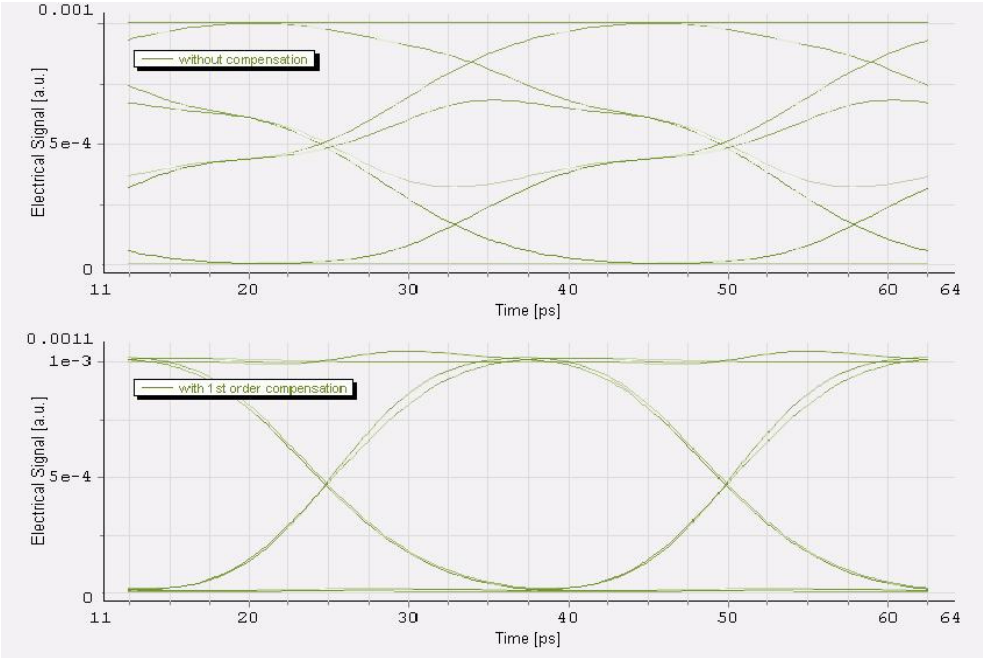

Figure 5.13 Eye Opening With or Without First Order Compensation @40Gbps with a Mean DGD value of ~10 ps

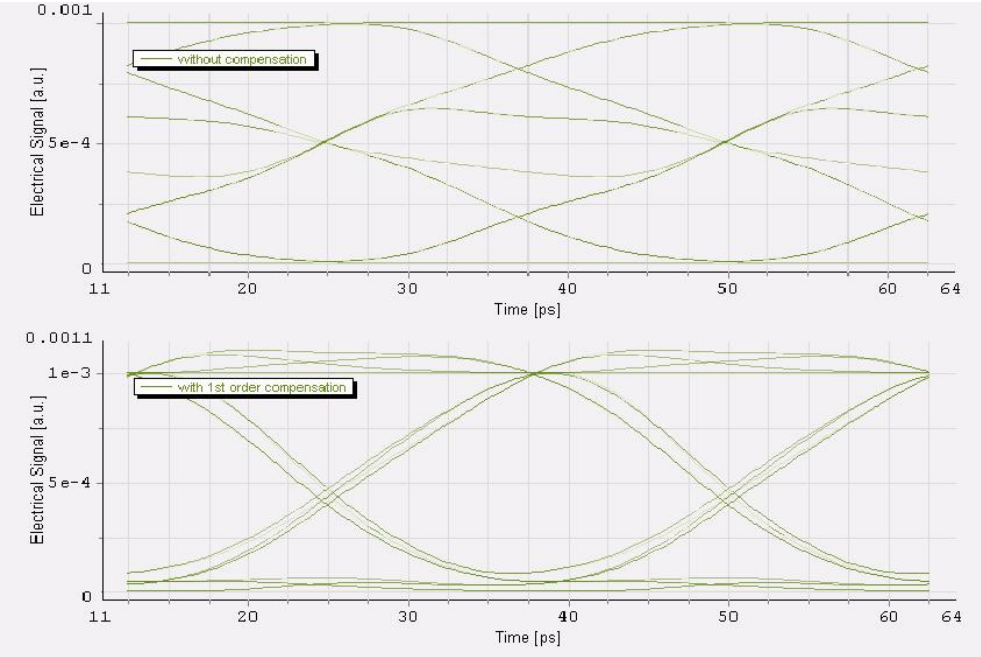

Figure 5.14 Eye Opening With or Without First Order Compensation @40Gbps with a Mean DGD value of ~15 ps

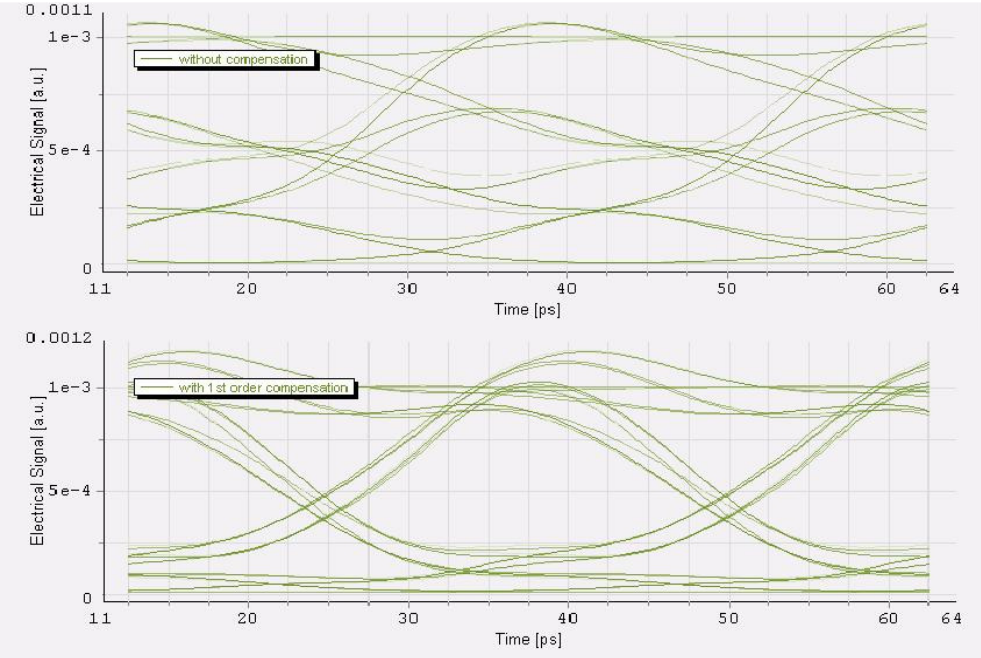

Figure 5.15 Eye Opening With or Without First Order Compensation @40Gbps with a Mean DGD value of ~20 ps

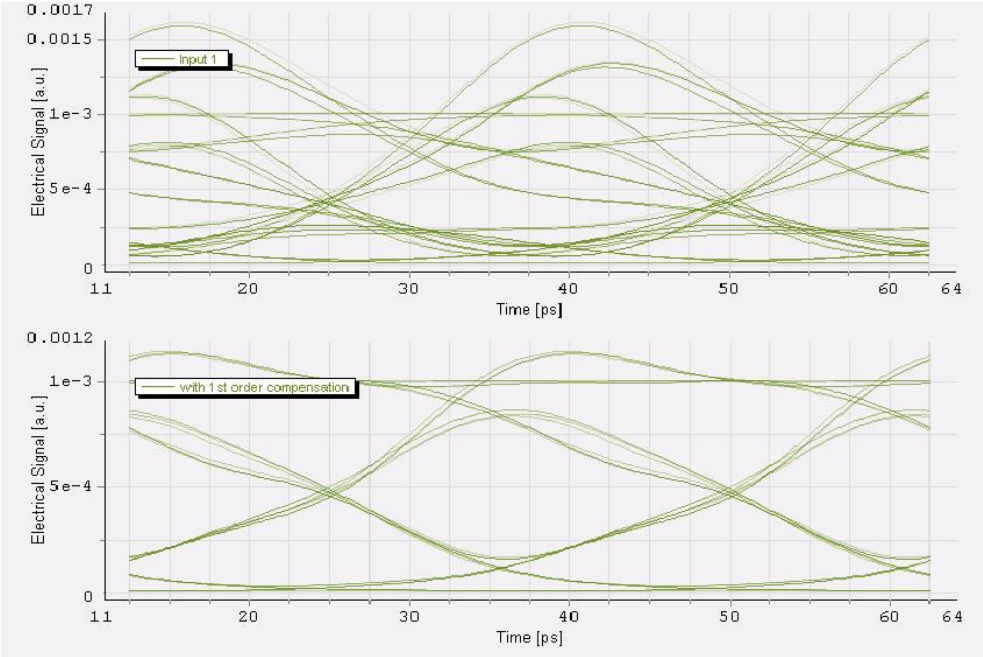

Figure 5.16 Eye Opening With or Without First Order Compensation @40Gbps with a Mean DGD value of ~25 ps

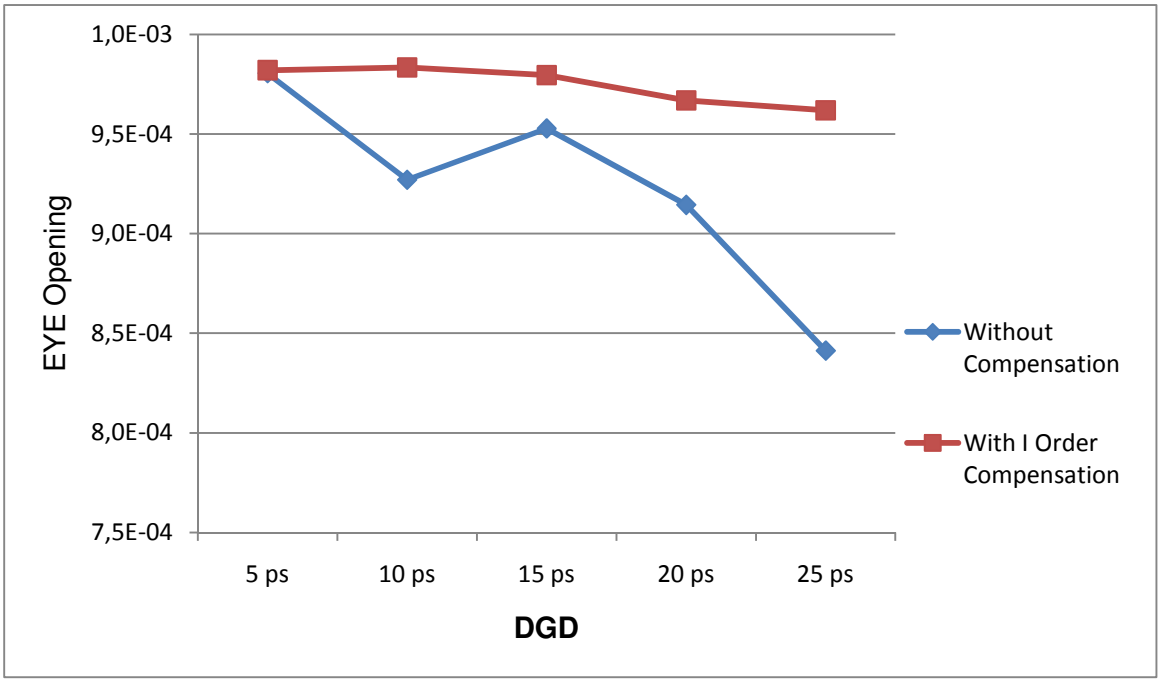

Figure 5.17 Simulation's results at 10 Gbps

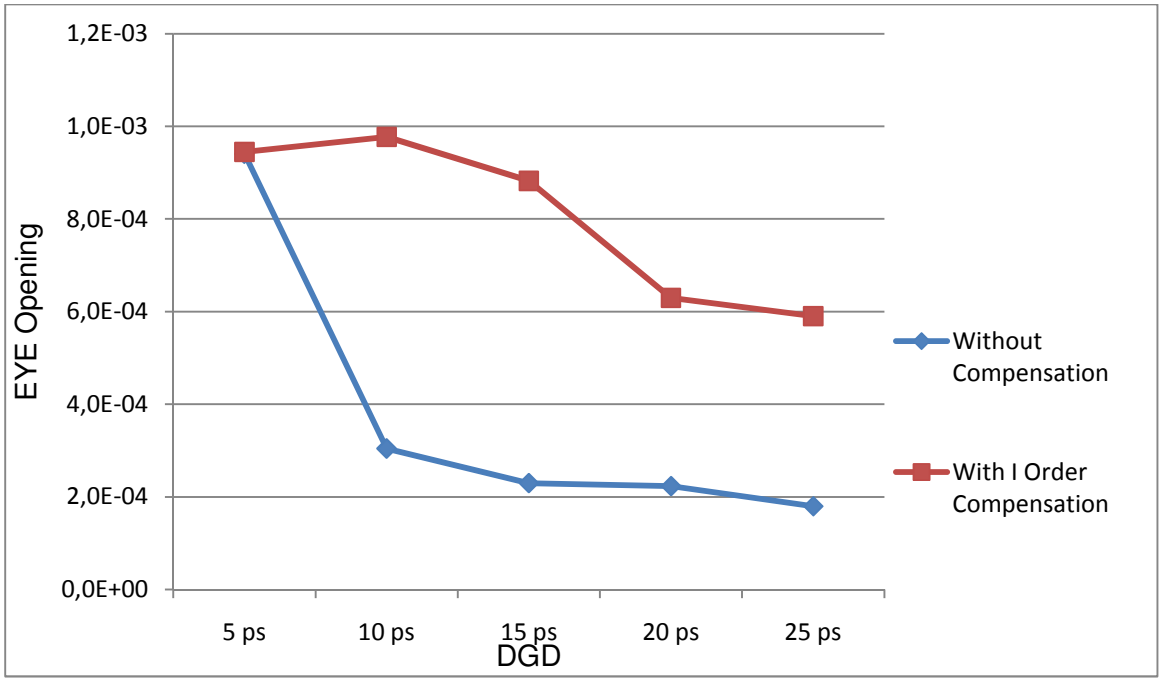

Figure 5.18 Simulation's results at 40 Gbps

The obtained PMD value at the end of the fiber varied from 5 to 25 ps with a step width of 5 ps, in order to obtain the performance of the compensator.

Figure from 5.7 to 5.16 shows a sequence of eye-diagram traces for the signal of Fig. 5.6 through the same fiber at the other end with and without PMD compensation at 10 and 40 Gbps.

The quality of the eye diagram is related to severity of PMD effects, the eye opening and quality of the eye diagram decrease as PMD value and the bit-rate get increased. As it can be seen from the eye diagrams, with the same value of PMD, the effects of this impairments are greater in the 40Gbps transmission. The results of the compensation performs always an increasing of the eye opening, but expecially for low value of DGD, it can be seen that the compensated signal perform an overcompensation that cause a distortion of the eye diagram.

5.3 Multi span compensation

After the investigation over the compensator's performance, is studied and reported how with the presence of a compensator it's possible to reach greater distances in the multi span system, studied in the second part of the previous chapter.

5.3.1 System setup

To compensate the signal at the output of the various fiber-loop amplifier, the scheme used in Section 4.1.3 was changed (Fig. 5.19) in order to store the data into a file, so that they can be read and analyzed by the compensator (fig. 5.2).

After the data generation, like in the previous section a compensation is performed.

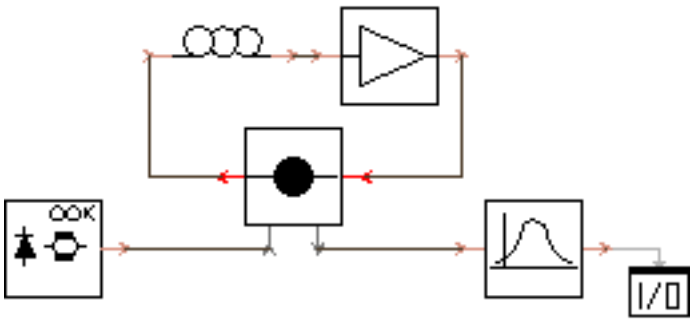

Figure 5.19 Modified schema

5.3.2 Simulation results and comments

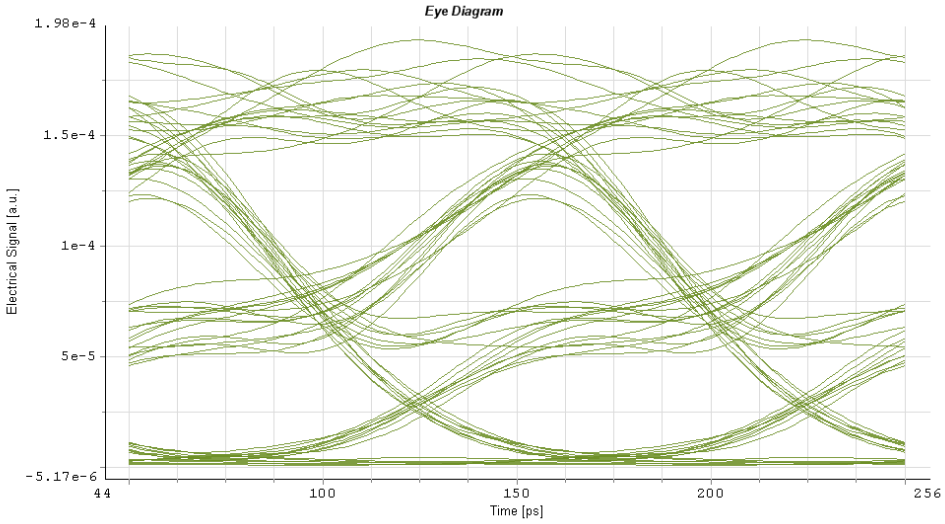

Figure 5.20 0.5 @10Gbps Without Compensation

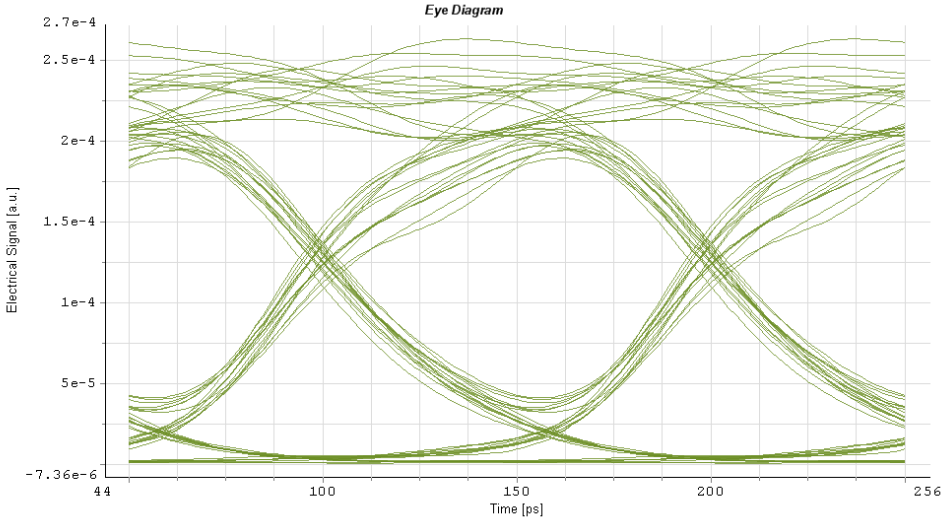

Figure 5.21 0.5 @10Gbps With Compensation

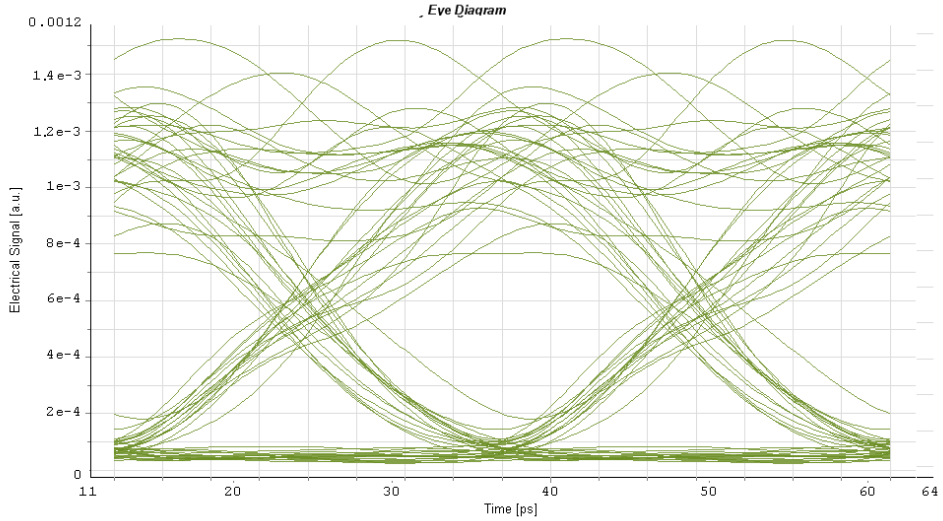

Figure 5.22 0.1 @10Gbps Without Compensation

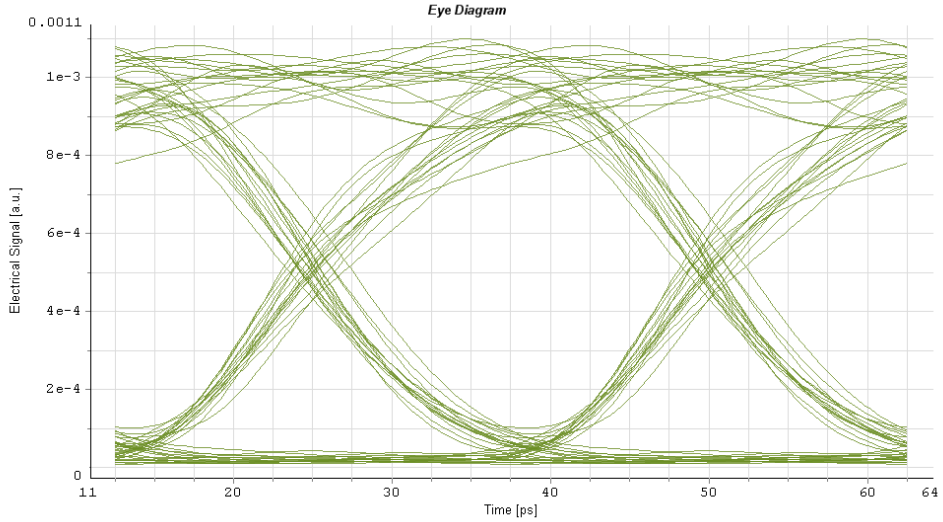

Figure 5.23 0.1 @10Gbps With Compensation

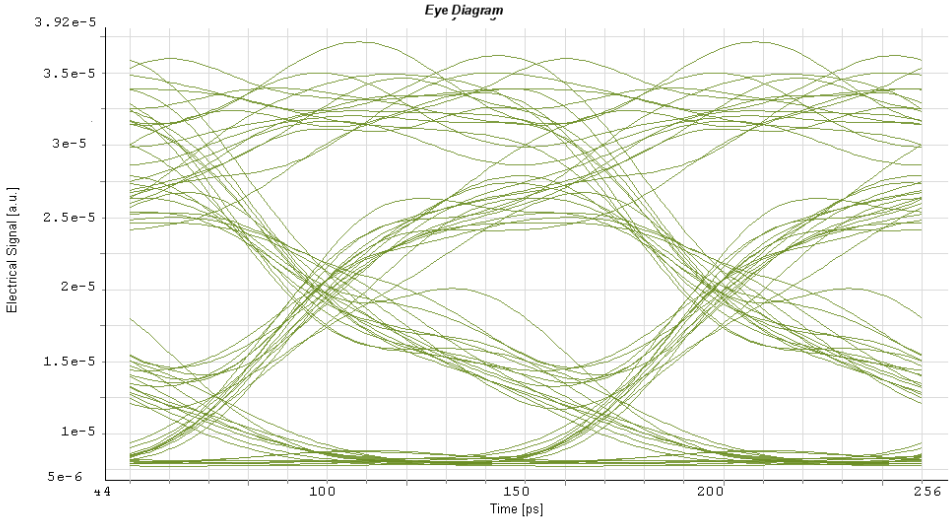

Figure 5.24 0.1 @40Gbps Without Compensation

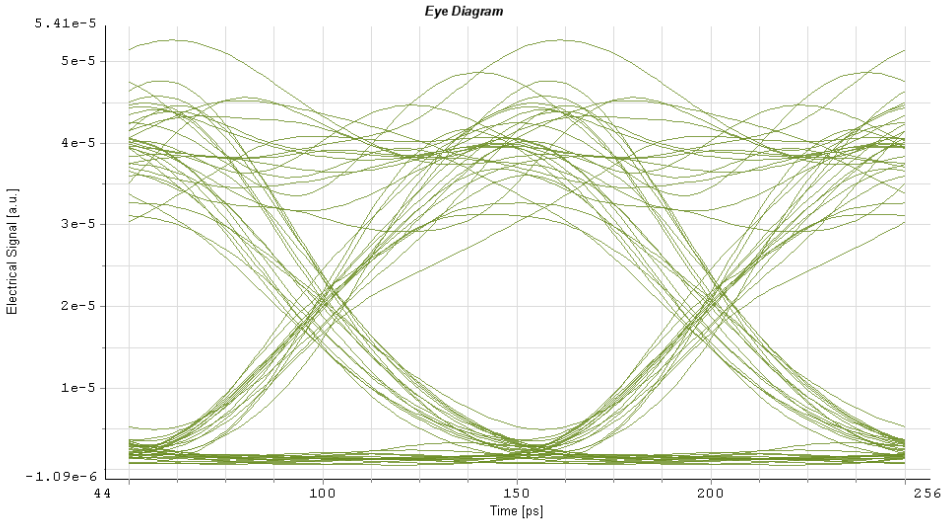

Figure 5.25 0.1 @40Gbps With Compensation

From the previous simulation the following data are extrapolated:

Bit Rate [Gbps]	PMD Coefficient $[^{ps}/_{\sqrt{Km}}]$	Max Length without compensation			Ber after compensation	Max Length with compensation [Km]	
		Max Length [Km]	Span Length [Km]	N° of span		Max Length [Km]	Span earned
10	0.5	450	50	9	10^{-16}	750	7
	0.1	1365	65	21	10^{-11}	1495	2
40	0.1	450	45	10	10^{-16}	675	5

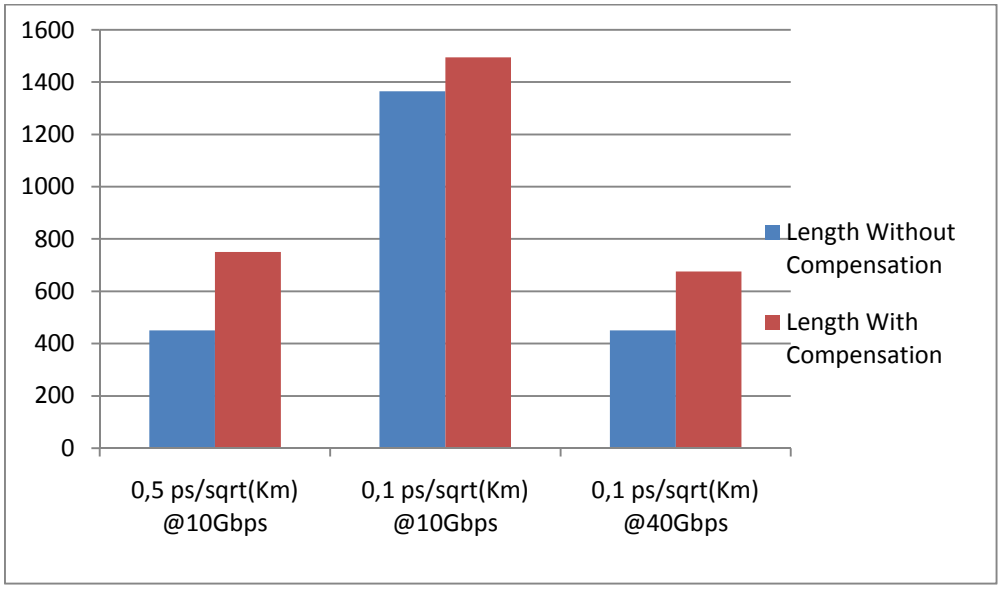

From the obtained data can be observed, how, using a compensator, is possible to achieve greater distances while minimizing the effect of PMD.

A 10 Gbps transmission with an high PMD coefficient it can be seen as it's not able to exceed 750 km, while a fiber with low PMD coefficient is able to match the performance of the fiber without the effect of PMD.

At 40 Gbps the limitations imposed by PMD are much higher, even in the case of fiber with low PMD coefficient (0.1 ps / km) which is barely more than half the length that reached without PMD influences in the fiber.

5.4 POWER PENALTY

After the investigation over the compensator efficiency, and the system improvement gave from the utilization of a PMD compensator in a communications system, we are going to study how a compensation can improve the system tolerance to the DGD.

5.4.1 Simulation Setup

At this point is analyzed how, with the use of a compensator, vary the system tolerance to the DGD, in the 40 Gbps system. The elaborated data are the one's created for the study over the compensator performaces.

To do that is added a power-meter at the end of the compensator's scheme, in order to monitorize the change of power, in function of the DGD value reached at the end of the fiber's link (Fig. 5.26).
The simulation starts by measuring the optical power received with a DGD value of , in order to set the 0 on the powers axis. Following the DGD values are increased until a 60% of the bit period. The obtained data are the results of the correlation between the DGD value and the power penalty at the receiver.

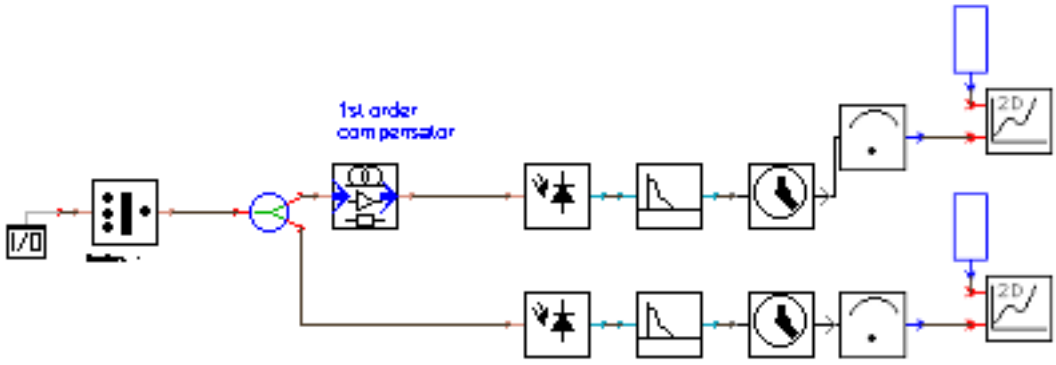

Figure 5.26 Power penalty setup

5.4.2 Results and discussion

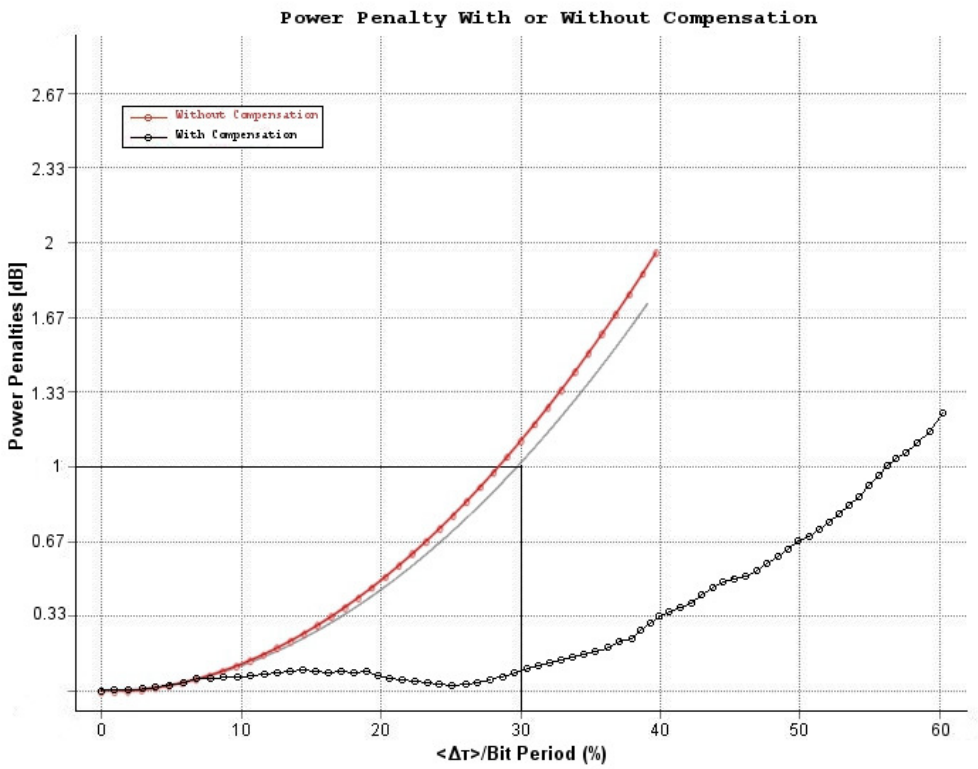

Figure 5.27 Power penalty with and without PMD compensation at 40Gbps

Fig. 5.27 shows the power penalty as a function of $\Delta\tau$ with and without PMD compensation. Here, γ is set to 0.5 assuming the worst possible waveform distortion caused by PMD. Without PMD compensation, the allowable $\Delta\tau$ for a penalty less than 1-dB (PMD tolerance) cannot overcame the 30% of the bit period instead of the compensated case, in which the allowable $\Delta\tau$, for not exceed a penalty of 1 dB, is the double with a limit of almost 60% of the bit period.

CHAPTER 6
CONCLUSION AND FUTURE WORKS

6.1 Conclusion

The work presented here is emphasized on the effects of Polarization Mode Dispersion (PMD) over the optical transmission.

The impacts produced by the increase of PMD and bit-rate are analyzed through eye diagrams, output power evaluation and ber estimation. Through the eye diagrams the output signal is observed at different values of PMD.

The second chapter provides an introduction to PMD. The causes of PMD and the role of birefringence were described in detail. The characterization of PMD using the differential group delay (DGD) concept and the principal states of polarization (PSP) model was explained. The effects of PMD, especially on digital optical communication systems (where PMD manifests as inter-symbol interference or ISI) were described, following which the need for compensating for PMD at 10 Gb/s and higher data rates was discussed.

The third chapter provided an overview of the existing PMD mitigation strategies. Their relative advantages and disadvantages were also mentioned. Optical PMD compensation strategies and electronic PMD mitigation techniques were individually taken-up and described. In addition to PMD compensation, steps to mitigate or overcome PMD, such as the use of PMD resistant modulation formats, were also described.

In the first simulative chapter, the impact of PMD on an optical communication system is studied. After a first investigation over the purely theoretical PMD limits at 10 an 40 Gbps, two more real ones are preformed. The results describe that PMD puts the hurdles to move to higher data rates, where puts a severe limits in transmission system with high PMD coefficient at 10 Gbps, until completely block a transmission at 40 Gbps; while, with a lower PMD coefficient, it starts to

seriously degraded the system performance at 40 Gbps; so a compensation is required to be able to transmit in those system.

The fifth chapter focused entirely on the adaptive PMD compensation system. After the presentation of the compensator setup, it's shown the monitor signal based on the Power Spectral Densities (PSD) and its performance in a 10 and 40 Gbps system.

A simulation over the PMD compensator is made, in order to evaluate its compensation capability in system at 10 and 40 Gbps with different value of DGD reached at the end of the fiber, from 5 to 25 ps with a step width of 5 ps; from the obtained results it can be seen how the eye diagram results more opened in comparison with the uncompensated one.
Then this setup is applied to the previous multispan system, where the maximum reachable length is improved.
In the last part of this chapter a study over the system tolerance over PMD is made; where it can be noted that the system tolerance is improved almost twice.

6.2 **Future work**

In this thesis is faced only the problem raised from first-order PMD effects, but with increasing bit rate also higher-order PMD played an important role in the optical system design. Also the compensator monitor is quite simple, and it isn't an automatic one because it doesn't have a control algorithm that controls automatically the polarization rotator and the delay line ; and the monitor suffers of a bit-rate dependency.

As future works, it can be improved the efficiency of the compensator taking in account the higher-order effects, implementing a more flexible and accurate feedback monitor, with an adequate control algorithm.

BIBLIOGRAPHY

1. **Di Ivan P. Kaminow, Thomas L. Koch.** *Optical fiber telecommunications III, Volume 1.* 1997.

2. **Heismann, F.** *Polarization Mode Dispersion: Fundamentals and Impact on Optical .* s.l. : Tutorial, Presented at European Conference on Optical , Sept. 1998.

3. *Polarization Mode Dispersion.* **Herwig Kogelnik, Robert M. Jopson, and Lynn E. Nelson.** s.l. : Optical Fiber Telecommunications, Elsevier Science, 2002, Vol. Volume IVB.

4. *PMD Vs Mode Coupling .* **Francis Audet.** s.l. : Exfo, Vol. Application Note 186.

5. *Polarization mode dispersion: time versus frequency domains.* **Pellaux, N. Gisin and J. P.** s.l. : Optics Communications 89, 1992.

6. *Phenomenological approach to Polarization dispersion in long single-mode fibers.* **Wagner, C. D. Poole and R. E.** s.l. : Electron. Lett., 1989, Vol. 22.

7. *PMD Second-Order Effects on Pulse Propagation in Single-Mode Optical Fibers.* **Cristian Francia, Frank Bruyère, Denis Penninckx, and Michel Chbat.** 12, s.l. : IEEE PHOTONICS TECHNOLOGY LETTERS, 1998, Vol. 10.

8. *Probability Densities of Second-Order Polarization Mode Dispersion Including Polarization Dependent Chromatic Fiber Dispersion.* **G. J. Foschini, L. E. Nelson, R. M. Jopson, and H. Kogelnik.** 3, s.l. : IEEE PHOTONICS TECHNOLOGY LETTERS, 2000, Vol. 12.

9. *Concatenation of polarization dispersion in single mode fibres.* **Curti.** 25, s.l. : Electronics Letters, 1989, Vol. .

10. **Poole, C. D., J. H. Winters and J. A. Nagel.** s.l. : Opt. Lett., 1991, Vol. 16.

11. *Testing Polarization Mode Dispersion (PMD) in the field.* **Lietaert, Gregor.** s.l. : JDSU, 2006.

12. **Poole, C. D.** 3, s.l. : IEE Phot. Tech, 1991.

13. *Automatic compensation technique for timewise fluctuating polarization mode dispersion in in-line amplifier systems.* **Takahashi, T., T. Imai, and M. Aiki.** s.l. : Electronics Letters.

14. *Analysis of signal degree of polarization degradation used as control signal for optical polarization mode dispersion compensation.* **Kikuchi, N.** s.l. : Journal of Lightwave Technology, 2001.

15. *Polarization-Mode Dispersion (PMD) detection sensitivity of degree of polarization method for PMD compensation.* **Kikuchi, N. and S. Sasaki.** s.l. : Proc. ECOC'99, 1999, Vol. II.

16. *Fast eye monitor for 10 Gbit/s and its application for optical PMD compensation.* **Buchali, F., S. Lanne, J.-P. Thiéry, W. Baumert and H. Bülow.** s.l. : Proc. OFC'2001, 2001.

17. *An adaptive first-order polarization-mode dispersion compensation system aided by polarization scrambling: theory and demonstration.* **Pua, H.Y., K. Peddanarappagari, B. Zhu, C. Allen, K. Demarest, and R. Hui.** 6, s.l. : Journal of Lightwave Technology, 2000, Vol. 18.

18. *"Polarization control method for suppressing polarization mode dispersion influence in optical transmission systems.* **Ono, T., S. Yamazaki, H. Shimizu, and K. Emura.** 5, s.l. : Journal of Lightwave Technology, 1994, Vol. 12.

19. *Higher order polarization mode dispersion compensator with three degrees of freedom.* **Karlsson. M., C. Xie, H. Sunnerud, and P.A. Andrekson.** s.l. : Proc. OFC'2001, 2001.

20. *A compensator for the effects of high-order polarization mode dispersion in optical fibers.* **Shtaif, M., A. Mecozzi, M. Tur, and J.A. Nagel.** 4, s.l. : IEEE Photonics Technology Letters, 2000, Vol. 12.

21. *Component for second-order compensation of polarization mode dispersion.* **Patscher, J. and R. Eckhardt.** 13, s.l. : Electronics Letters, 1997, Vol. 3.

22. *PMD Compensation/Mitigation Techniques for High-Speed Optical Transport.* **Henning Bülow, Chongjin Xie, Axel Klekamp, Xiang Liu, and Bernd Franz.** s.l. : Bell Labs Technical Journal , 2009.

23. *Enhanced PMD mitigation using forward-error-correction coding and a first-order compensator.* **Xie, Y., Q. Yu, L.-S. Yan, O. H. Adamczyk, Z. Pan, S. Lee, A. E. Willner and C. R. Menyuk.** s.l. : Proc. OFC'2001, 2001.

24. *"Comparison of different modulation formats in terrestrial systems with high polarization mode dispersion.* **Khosravani, R. and A. E. Willner.** Bartimora : PROC OFC 2000, 2000.

25. *"Comparison of resistance to polarization mode dispersion of NRZ and phase-shaped binary transmission formats at 10 Gbit7s.* **Pierre. L. and, J.-P. Thiery.** 5, s.l. : Electronics Letters, 1997, Vol. 33.

26. *First-order polarization-mode dispersion adaptive compensation system.* **Pua, H.Y.** University of Kansas : s.n., 1998.

27. *PMD fundamentals: Polarization mode dispersion in optical fibers.* **Kogelnik, J. P. Gordon and H.** s.l. : Bell Laboratories, 2000.

28. *dfggdgdfg.* **ertertrdeg, fgh fghhfd.** 333, sdesreg, pp. 54-59.